(12) INTERNATIONAL APPLICATION PUBLISHED UNDER THE PATENT COOPERATION TREATY (PCT)

(19) World Intellectual Property Organization
International Bureau

(43) International Publication Date
22 June 2023 (22.06.2023)

WIPO | PCT

(10) International Publication Number
WO 2023/111173 A1

(51) International Patent Classification:
A61K 31/4155 (2006.01) *A61K 9/00* (2006.01)
A61K 31/496 (2006.01) *A61P 35/02* (2006.01)
A61K 45/06 (2006.01)

(21) International Application Number:
PCT/EP2022/086142

(22) International Filing Date:
15 December 2022 (15.12.2022)

(25) Filing Language: English

(26) Publication Language: English

(30) Priority Data:
21306789.5 16 December 2021 (16.12.2021) EP

(71) Applicants: **INSERM (INSTITUT NATIONAL DE LA SANTÉ ET DE LA RECHERCHE MÉDICALE)** [FR/FR]; 101, rue de Tolbiac, 75013 Paris (FR). **UNIVERSITÉ D'AIX MARSEILLE** [FR/FR]; 58 Boulevard Charles Livon, 13007 MARSEILLE (FR). **CENTRE NATIONAL DE LA RECHERCHE SCIENTIFIQUE** [FR/FR]; 3, Rue Michel Ange, 75016 Paris (FR). **INSTITUT JEAN PAOLI & IRENE CALMETTES** [FR/FR]; 232 Boulevard Sainte-Marguerite, 13009 Marseille (FR).

(72) Inventors: **DUPREZ, Estelle**; INSTITUT PAOLI-CALMETTES - U1068 27 BOULEVARD LEI ROURE, 13273 MARSEILLE CEDEX 09 (FR). **POPLINEAU, Mathilde**; CRCT - U1037 2 AVENUE HUBERT CURIEN, 31037 TOULOUSE CEDEX 1 (FR).

(74) Agent: **INSERM TRANSFERT**; 7 rue Watt, 75013 Paris (FR).

(81) Designated States *(unless otherwise indicated, for every kind of national protection available)*: AE, AG, AL, AM, AO, AT, AU, AZ, BA, BB, BG, BH, BN, BR, BW, BY, BZ, CA, CH, CL, CN, CO, CR, CU, CV, CZ, DE, DJ, DK, DM, DO, DZ, EC, EE, EG, ES, FI, GB, GD, GE, GH, GM, GT, HN, HR, HU, ID, IL, IN, IQ, IR, IS, IT, JM, JO, JP, KE, KG, KH, KN, KP, KR, KW, KZ, LA, LC, LK, LR, LS, LU, LY, MA, MD, MG, MK, MN, MW, MX, MY, MZ, NA, NG, NI, NO, NZ, OM, PA, PE, PG, PH, PL, PT, QA, RO, RS, RU, RW, SA, SC, SD, SE, SG, SK, SL, ST, SV, SY, TH, TJ, TM, TN, TR, TT, TZ, UA, UG, US, UZ, VC, VN, WS, ZA, ZM, ZW.

(84) Designated States *(unless otherwise indicated, for every kind of regional protection available)*: ARIPO (BW, CV, GH, GM, KE, LR, LS, MW, MZ, NA, RW, SD, SL, ST, SZ, TZ, UG, ZM, ZW), Eurasian (AM, AZ, BY, KG, KZ, RU, TJ, TM), European (AL, AT, BE, BG, CH, CY, CZ, DE, DK, EE, ES, FI, FR, GB, GR, HR, HU, IE, IS, IT, LT, LU, LV, MC, ME, MK, MT, NL, NO, PL, PT, RO, RS, SE, SI, SK, SM, TR), OAPI (BF, BJ, CF, CG, CI, CM, GA, GN, GQ, GW, KM, ML, MR, NE, SN, TD, TG).

Published:
— *with international search report (Art. 21(3))*
— *in black and white; the international application as filed contained color or greyscale and is available for download from PATENTSCOPE*

(54) Title: AN EZH2 DEGRADER OR INHIBITOR FOR USE IN THE TREATMENT OF RESISTANT ACUTE MYELOID LEUKEMIA

(57) Abstract: The present invention relates to the treatment of resistant leukemia. The inventor studied APL cellular heterogeneity by integrating scRNA-seq and scATAC-seq data obtained from PLZF-RARA transformed promyelocytes treated with RA. Establishing cellular clusters and arranging them in hierarchies helped them to identify a subpopulation of transformed promyelocytes that were insensitive to RA-induced differentiation and characterized by a DNA repair gene expression signature and high expression of Enhancer of Zeste Homolog 2 (EZH2), the catalytic subunit of Polycomb Repressive Complex 2 (PRC2). Because EZH2 contribution to the pathogenesis of leukemia is contrasted, they further explored EZH2 function in APL development and RA treatment response. They discovered a dual role of EZH2 in APL onset and RA response, suggesting the need to target the non-histone methyltransferase activity of EZH2 for leukemia clearance. Particularly, they showed that the use of an EZH2-selective degrader significantly reduced growth and viability of PLZF-RARA expressing leukemic cells and increased the survival of the mice transplanted with pre-treated leukemia. Thus, the present invention relates to an EZH2 degrader or an inhibitor of the EZH2 gene expression for use in the treatment of resistant leukemia in a patient in need thereof.

WO 2023/111173 A1

AN EZH2 DEGRADER OR INHIBITOR FOR USE IN THE TREATMENT OF RESISTANT ACUTE MYELOID LEUKEMIA

FIELD OF THE INVENTION:

The present invention relates to an EZH2 degrader or an inhibitor of the EZH2 gene expression for use in the treatment of resistant leukemia in a patient in need thereof.

BACKGROUND OF THE INVENTION:

Acute myeloid leukemia (AML), characterized by clonal growth and evolution of an undifferentiated hematopoietic cell is a heterogeneous disease in terms of cell-of-origin, genetic and epigenetic alterations, clinical features and treatment outcomes (Papaemmanuil et al., 2016); (Bullinger et al., 2017). Yet, recurrent chromosomal rearrangements leading to the generation of oncogenic fusion proteins are common in AML and an abundant literature has emphasized their driver role in its development and response to therapeutics (Brien et al., 2019).

Acute promyelocytic leukemia (APL) is a class of AML that accounts for 10–15% of all cases and is characterized by recurrent chromosomal translocations involving invariably the gene encoding the Retinoic Acid Receptor alpha (RARA) (17q21) with several fusion partners, such as PML (15q22) or PLZF (11q23) (For review (Dos Santos et al., 2013)). The resulting fusion proteins behave as RARA signaling repressors due to their ability to oligomerize and to recruit epigenetic repressors at cis-regulatory DNA regions of RARA target genes and initiate oncogenic gene expression signatures (Grignani et al., 1993) and X-RARA fusion proteins were among the first transcription factors to be identified as drivers of cancer (Di Croce, 2005).

In the case of APL patients with PML-RARA fusion, this oncogenic activity can be overcome by pharmacological levels of RA, which induces APL blast differentiation and patient complete remission (Huang et al., 1988); (de The and Chen, 2010). This exquisite RA sensitivity has made APL one of the most successful examples of targeted therapy to mutational events (Tallman, 2004); (de The et al., 2017). However, resistance to single agent therapies is a frequent event (Holohan et al., 2013) and although very successfully advanced, RA-targeted-treatment of APL still poses clinical challenges. Indeed, it has been reported that among the PML-RARA patients a high-risk entity exists, characterized by a higher relapse rate with RA-resistance (Jimenez et al., 2020). RA resistance is also the problem of APL patients with t(11;17) bearing the PLZF-RARA fusion protein, which respond poorly to RA and remain clinically resistant (Sobas et al., 2020). Contrary to PML-RARA APL, pharmacological doses of RA, although inducing partial differentiation of the PLZF-RARA blasts do not clear the

Leukemia Initiating cell (LIC) of this APL variant (Nasr et al., 2008); (Ablain et al., 2014). This highlighted the uncoupling between blast differentiation and tumor eradication and shed light on other biological processes such as senescence and proteolysis whose activation seems to be a key to cure APL (Ablain et al., 2014). To identify vulnerabilities that will prevent resistance and facilitate treatment response, much work has been done to understand the cellular and molecular bases of PLZF-RARA APL physiopathology (Noguera et al., 2019). The PLZF moiety of the fusion is thought to play a determinant role in RA-resistance. PLZF is a potent transcriptional repressor that can interact by itself with epigenetic complexes (He et al., 1998); (Grignani et al., 1998). Given that PLZF binding sites with corepressors are conserved in the PLZF-RARA fusion, one hypothesis is that inappropriate recruitment of functional epigenetic repressors, such as the polycomb repressor complex 1 (PRC1), would trigger epigenetic imbalance at very specific genomic loci in an RA insensitive manner (Boukarabila et al., 2009). This is consistent with the observed degradation of PLZF-RARA under RA treatment (Rego et al., 2000) suggesting a persistent mechanism even in the absence of detectable fusion involving chromatin modifications. However, the molecular basis for the resistance of PLZF-RARA expressing cells and why some cells retain their self-renewal capacity while others do not after RA treatment remain unknown.

SUMMARY OF THE INVENTION:

To advance in the understanding of RA resistance, the inventor studied APL cellular heterogeneity by integrating scRNA-seq and scATAC-seq data obtained from PLZF-RARA transformed promyelocytes treated with RA. Establishing cellular clusters and arranging them in hierarchies helped them to identify a subpopulation of transformed promyelocytes that were insensitive to RA-induced differentiation and characterized by a DNA repair gene expression signature and high expression of Enhancer of Zeste Homolog 2 (EZH2), the catalytic subunit of Polycomb Repressive Complex 2 (PRC2). Because EZH2 contribution to the pathogenesis of leukemia is contrasted (Basheer et al., 2019), they further explored EZH2 function in APL development and RA treatment response. They discovered a dual role of EZH2 in APL onset and RA response, suggesting the need to target the non-histone methyltransferase activity of EZH2 for leukemia clearance. Particularly, they showed that the use of an EZH2-selective degrader significantly reduced growth and viability of PLZF-RARA expressing leukemic cells and increased the survival of the mice transplanted with pre-treated leukemia.

Thus, the present invention relates to an EZH2 degrader or an inhibitor of the EZH2 gene expression for use in the treatment of resistant leukemia in a patient in need thereof. Particularly, the invention is defined by its claims.

DETAILED DESCRIPTION OF THE INVENTION:

In a first aspect, the invention relates to an EZH2 degrader or an inhibitor of the EZH2 gene expression for use in the treatment of resistant leukemia in a patient in need thereof.

In other words, the invention relates to an EZH2 degrader or an inhibitor of the EZH2 gene expression for use to sensitize resistant cancerous cells to therapeutic compounds used to treat leukemia like RA.

In other words, the invention relates to an EZH2 degrader or an inhibitor of the EZH2 gene expression to sensitize resistant leukemia cancerous cells to therapeutic compounds used to treat leukemia.

In another particular embodiment, the invention relates to an i) EZH2 degrader or an inhibitor of the EZH2 gene expression and a ii) therapeutic compound already used to treat leukemia according to the invention as a combined preparation for simultaneous, separate or sequential use in the treatment of resistant leukemia or use in the sensitization of resistant leukemia cancerous cells.

In a particular embodiment, the resistant leukemia is a resistant acute lymphocytic leukemia (ALL) or a resistant acute myeloid leukemia (AML).

In a particular embodiment, the resistant leukemia is a resistant acute promyelocytic leukemia (APL), a resistant PLZF-RARA acute promyelocytic leukemia (APL), a resistant cytogenetically normal AML (CN-AML), a resistant acute myeloid leukemia with trisomy 8 or a resistant acute leukemia with MLL translocations.

In one embodiment, the resistant APL cells express the PLZF-RARA fusion protein due to the translocation t(11;17)(q23;q21).

Thus, the invention also relates to an EZH2 degrader or an inhibitor of the EZH2 gene expression for use in the treatment of a resistant acute promyelocytic leukemia (APL) in a patient in need thereof.

In a particular embodiment, the invention relates to an EZH2 degrader or an inhibitor of the EZH2 gene expression for use in the treatment of resistant acute promyelocytic leukemia (APL) in a patient in need thereof.

According to the invention, leukemia of the invention like AML or APL are resistant to Retinoic Acid (RA) and for example to the all-trans retinoic acid (ATRA) or to the tretinoin.

As used herein, the term “resistant leukemia” denotes a leukemia which will resist or not respond to classical treatment or therapeutic compounds already used to treat such diseases.

As used herein and according to the invention, classical treatment or therapeutic compounds already used to treat leukemia can be for example all-trans retinoic acid (ATRA; tretinoin), gemtuzumab ozogamicin, the combination of methotrexate, mercaptopurine and ATRA, demethylating agent, or chemotherapy such as cytarabine (araC), docetaxel, etoposide, idarubicin, volasertib, tozasertib (VX-680), nutlin 3, Olaparib or allograft.

Compounds useful for the treatment of leukemia are well known in the art (see for example Sweet K. et al., 2014).

As used herein, the term “chemotherapy” refers to use of chemotherapeutic agents to treat a subject. As used herein, the term "chemotherapeutic agent" or “anti-cancer agents” refers to chemical compounds that are effective in inhibiting tumor growth.

In some embodiment, the therapeutic compounds used to treat leukemia are chemotherapeutic agents.

In some embodiment, the therapeutic compounds used to treat leukemia is selected from cytarabine (araC), volasertib, tozasertib (VX-680), nutlin 3 or olaparib.

As used herein, the term “EZH2” denotes a histone-lysine N-methyltransferase enzyme (EC 2.1.1.43) encoded by EZH2 gene, that participates in histone methylation and, ultimately, transcriptional repression. EZH2 catalyzes the addition of methyl groups to histone H3 at lysine 27, by using the cofactor S-adenosyl-L-methionine. Methylation activity of EZH2 facilitates heterochromatin formation thereby silences gene function. Remodeling of chromosomal heterochromatin by EZH2 is also required during cell mitosis. Its Entrez access gene number is 2146.

In some embodiments, the invention relates to an EZH2 degrader for use in the treatment of resistant leukemia in a patient in need thereof. In some embodiments, the invention relates to an EZH2 degrader for use in the treatment of resistant acute promyelocytic leukemia in a patient in need thereof. As used herein the term “degrader” denotes a molecule capable of degrading another one by using the proteasome system of the cells. It results that the molecule

targeted by the degrader is not visible. A degrader according to the invention can also be a PROTAC (proteolysis targeting chimeras).

Thus, as used herein the term “EZH2 degrader” denotes a molecule capable of degrading EZH2 in a cell and particularly in resistant leukemia cells according to the invention. As example, an enzyme inhibiting the activity of EZH2 is not considered as an EHZ2 degrader since it is not a molecule capable of degrading EZH2 by using the proteasome system of the cells. In the present disclosure, it is demonstrated that the oncogenic activity of EZH2 is not solely based on its catalytic activity and that EZH2 degraders are relevant for the treatment of cancers dependent on non-catalytic (non-canonical) activity of EZH2.

As used herein, the term “patient” denotes a mammal, such as a rodent, a feline, a canine, and a primate. Particularly, the patient according to the invention is a human.

As used herein, the term "treatment" or "treat" refer to both prophylactic or preventive treatment as well as curative or disease modifying treatment, including treatment of patients at risk of contracting the disease or suspected to have contracted the disease as well as patients who are ill or have been diagnosed as suffering from a disease or medical condition, and includes suppression of clinical relapse. The treatment may be administered to a patient having a medical disorder or who ultimately may acquire the disorder, in order to prevent, cure, delay the onset of, reduce the severity of, or ameliorate one or more symptoms of a disorder or recurring disorder, or in order to prolong the survival of a patient beyond that expected in the absence of such treatment. By "therapeutic regimen" is meant the pattern of treatment of an illness, e.g., the pattern of dosing used during therapy. A therapeutic regimen may include an induction regimen and a maintenance regimen. The phrase "induction regimen" or "induction period" refers to a therapeutic regimen (or the portion of a therapeutic regimen) that is used for the initial treatment of a disease. The general goal of an induction regimen is to provide a high level of drug to a patient during the initial period of a treatment regimen. An induction regimen may employ (in part or in whole) a "loading regimen", which may include administering a greater dose of the drug than a physician would employ during a maintenance regimen, administering a drug more frequently than a physician would administer the drug during a maintenance regimen, or both. The phrase "maintenance regimen" or "maintenance period" refers to a therapeutic regimen (or the portion of a therapeutic regimen) that is used for the maintenance of a patient during treatment of an illness, e.g., to keep the patient in remission for long periods of time (months or years). A maintenance regimen may employ continuous therapy

(e.g., administering a drug at regular intervals, e.g., weekly, monthly, yearly, etc.) or intermittent therapy (e.g., interrupted treatment, intermittent treatment, treatment at relapse, or treatment upon achievement of a particular predetermined criteria [e.g., disease manifestation, etc.]).

In one embodiment, the degrader according to the invention may be a low molecular weight compound, e. g. a small organic molecule (natural or not).

The term "small organic molecule" refers to a molecule (natural or not) of a size comparable to those organic molecules generally used in pharmaceuticals. The term excludes biological macromolecules (e. g., proteins, nucleic acids, etc.). Preferred small organic molecules range in size up to about 10000 Da, more preferably up to 5000 Da, more preferably up to 2000 Da and most preferably up to about 1000 Da.

In one embodiment, the EZH2 degrader is the molecule MS1943 of formula I (see also Ma et al., 2020):

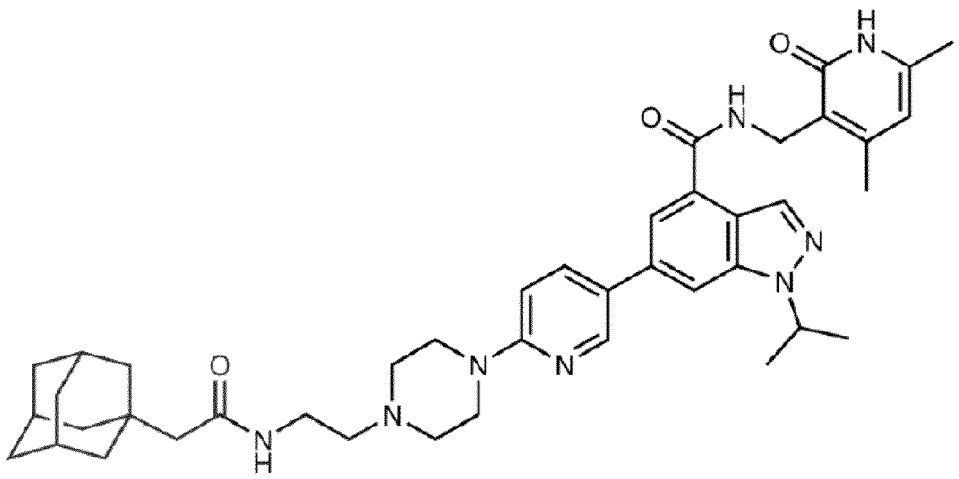

MS1943 (1)

In another embodiment, the EZH2 degrader (EZH2 PROTAC) can be a molecule as described in Liu, Z. et 2021.

In one embodiment, the degrader according to the invention is a polypeptide.

In a particular embodiment the polypeptide is a decoy receptor of EZH2 and is capable to capture the enzyme EZH2.

In one embodiment, the polypeptide of the invention may be linked to a cell-penetrating peptide" to allow the penetration of the polypeptide in the cell.

The term "cell-penetrating peptides" are well known in the art and refers to cell permeable sequence or membranous penetrating sequence such as penetratin, TAT mitochondrial penetrating sequence and compounds (Bechara and Sagan, 2013; Jones and Sayers, 2012; Khafagy el and Morishita, 2012; Malhi and Murthy, 2012).

The polypeptides of the invention may be produced by any suitable means, as will be apparent to those of skill in the art. In order to produce sufficient amounts of polypeptide or functional equivalents thereof for use in accordance with the present invention, expression may conveniently be achieved by culturing under appropriate conditions recombinant host cells containing the polypeptide of the invention. Preferably, the polypeptide is produced by recombinant means, by expression from an encoding nucleic acid molecule. Systems for cloning and expression of a polypeptide in a variety of different host cells are well known.

When expressed in recombinant form, the polypeptide is preferably generated by expression from an encoding nucleic acid in a host cell. Any host cell may be used, depending upon the individual requirements of a particular system. Suitable host cells include bacteria mammalian cells, plant cells, yeast and baculovirus systems. Mammalian cell lines available in the art for expression of a heterologous polypeptide include Chinese hamster ovary cells. HeLa cells, baby hamster kidney cells and many others. Bacteria are also preferred hosts for the production of recombinant protein, due to the ease with which bacteria may be manipulated and grown. A common, preferred bacterial host is E coli.

In specific embodiments, it is contemplated that polypeptides used in the therapeutic methods of the present invention may be modified in order to improve their therapeutic efficacy. Such modification of therapeutic compounds may be used to decrease toxicity, increase circulatory time, or modify biodistribution. For example, the toxicity of potentially important therapeutic compounds can be decreased significantly by combination with a variety of drug carrier vehicles that modify biodistribution. In example adding dipeptides can improve the penetration of a circulating agent in the eye through the blood retinal barrier by using endogenous transporters.

A strategy for improving drug viability is the utilization of water-soluble polymers. Various water-soluble polymers have been shown to modify biodistribution, improve the mode of cellular uptake, change the permeability through physiological barriers; and modify the rate of clearance from the body. To achieve either a targeting or sustained-release effect, water-

soluble polymers have been synthesized that contain drug moieties as terminal groups, as part of the backbone, or as pendent groups on the polymer chain.

Polyethylene glycol (PEG) has been widely used as a drug carrier, given its high degree of biocompatibility and ease of modification. Attachment to various drugs, proteins, and liposomes has been shown to improve residence time and decrease toxicity. PEG can be coupled to active agents through the hydroxyl groups at the ends of the chain and via other chemical methods; however, PEG itself is limited to at most two active agents per molecule. In a different approach, copolymers of PEG and amino acids were explored as novel biomaterials which would retain the biocompatibility properties of PEG, but which would have the added advantage of numerous attachment points per molecule (providing greater drug loading), and which could be synthetically designed to suit a variety of applications.

Those of skill in the art are aware of PEGylation techniques for the effective modification of drugs. For example, drug delivery polymers that consist of alternating polymers of PEG and tri-functional monomers such as lysine have been used by VectraMed (Plainsboro, N.J.). The PEG chains (typically 2000 daltons or less) are linked to the a- and e-amino groups of lysine through stable urethane linkages. Such copolymers retain the desirable properties of PEG, while providing reactive pendent groups (the carboxylic acid groups of lysine) at strictly controlled and predetermined intervals along the polymer chain. The reactive pendent groups can be used for derivatization, cross-linking, or conjugation with other molecules. These polymers are useful in producing stable, long-circulating pro-drugs by varying the molecular weight of the polymer, the molecular weight of the PEG segments, and the cleavable linkage between the drug and the polymer. The molecular weight of the PEG segments affects the spacing of the drug/linking group complex and the amount of drug per molecular weight of conjugate (smaller PEG segments provides greater drug loading). In general, increasing the overall molecular weight of the block co-polymer conjugate will increase the circulatory half-life of the conjugate. Nevertheless, the conjugate must either be readily degradable or have a molecular weight below the threshold-limiting glomular filtration (e.g., less than 60 kDa).

In addition, to the polymer backbone being important in maintaining circulatory half-life, and biodistribution, linkers may be used to maintain the therapeutic agent in a pro-drug form until released from the backbone polymer by a specific trigger, typically enzyme activity in the targeted tissue. For example, this type of tissue activated drug delivery is particularly useful where delivery to a specific site of biodistribution is required and the therapeutic agent is released at or near the site of pathology. Linking group libraries for use in activated drug delivery are known to those of skill in the art and may be based on enzyme kinetics, prevalence

of active enzyme, and cleavage specificity of the selected disease-specific enzymes. Such linkers may be used in modifying the protein or fragment of the protein described herein for therapeutic delivery.

In another embodiment, the invention also relates to an inhibitor of the EZH2 gene expression.

As used herein, the term "inhibitor of the EZH2 gene expression." denotes inhibitor of the expression of the gene coding for the EZH2 protein like for example siRNA or shRNA.

Small inhibitory RNAs (siRNAs) can also function as inhibitors of EZH2 gene expression for use in the present invention. EZH2 gene expression can be reduced by contacting a patient or cell with a small double stranded RNA (dsRNA), or a vector or construct causing the production of a small double stranded RNA, such that EZH2 gene expression is specifically inhibited (i.e. RNA interference or RNAi). Methods for selecting an appropriate dsRNA or dsRNA-encoding vector are well known in the art for genes whose sequence is known (e.g. see for example Tuschl, T. et al. (1999); Elbashir, S. M. et al. (2001); Hannon, GJ. (2002); McManus, MT. et al. (2002); Brummelkamp, TR. et al. (2002); U.S. Pat. Nos. 6,573,099 and 6,506,559; and International Patent Publication Nos. WO 01/36646, WO 99/32619, and WO 01/68836).

Ribozymes can also function as inhibitors of EZH2 gene expression for use in the present invention. Ribozymes are enzymatic RNA molecules capable of catalyzing the specific cleavage of RNA. The mechanism of ribozyme action involves sequence specific hybridization of the ribozyme molecule to complementary target RNA, followed by endonucleolytic cleavage. Engineered hairpin or hammerhead motif ribozyme molecules that specifically and efficiently catalyze endonucleolytic cleavage of EZH2 mRNA sequences are thereby useful within the scope of the present invention. Specific ribozyme cleavage sites within any potential RNA target are initially identified by scanning the target molecule for ribozyme cleavage sites, which typically include the following sequences, GUA, GUU, and GUC. Once identified, short RNA sequences of between about 15 and 20 ribonucleotides corresponding to the region of the target gene containing the cleavage site can be evaluated for predicted structural features, such as secondary structure, that can render the oligonucleotide sequence unsuitable. The suitability of candidate targets can also be evaluated by testing their accessibility to hybridization with complementary oligonucleotides, using, e.g., ribonuclease protection assays.

Both antisense oligonucleotides and ribozymes useful as inhibitors of EZH2 gene expression can be prepared by known methods. These include techniques for chemical synthesis

such as, e.g., by solid phase phosphoramadite chemical synthesis. Alternatively, anti-sense RNA molecules can be generated by in vitro or in vivo transcription of DNA sequences encoding the RNA molecule. Such DNA sequences can be incorporated into a wide variety of vectors that incorporate suitable RNA polymerase promoters such as the T7 or SP6 polymerase promoters. Various modifications to the oligonucleotides of the invention can be introduced as a means of increasing intracellular stability and half-life. Possible modifications include but are not limited to the addition of flanking sequences of ribonucleotides or deoxyribonucleotides to the 5' and/or 3' ends of the molecule, or the use of phosphorothioate or 2'-O-methyl rather than phosphodiesterase linkages within the oligonucleotide backbone.

Antisense oligonucleotides siRNAs and ribozymes of the invention may be delivered in vivo alone or in association with a vector. In its broadest sense, a "vector" is any vehicle capable of facilitating the transfer of the antisense oligonucleotide siRNA or ribozyme nucleic acid to the cells and preferably cells expressing EZH2. Preferably, the vector transports the nucleic acid to cells with reduced degradation relative to the extent of degradation that would result in the absence of the vector. In general, the vectors useful in the invention include, but are not limited to, plasmids, phagemids, viruses, other vehicles derived from viral or bacterial sources that have been manipulated by the insertion or incorporation of the antisense oligonucleotide siRNA or ribozyme nucleic acid sequences. Viral vectors are a preferred type of vector and include, but are not limited to nucleic acid sequences from the following viruses: retrovirus, such as moloney murine leukemia virus, harvey murine sarcoma virus, murine mammary tumor virus, and rouse sarcoma virus; adenovirus, adeno-associated virus; SV40-type viruses; polyoma viruses; Epstein-Barr viruses; papilloma viruses; herpes virus; vaccinia virus; polio virus; and RNA virus such as a retrovirus. One can readily employ other vectors not named but known to the art.

Preferred viral vectors are based on non-cytopathic eukaryotic viruses in which non-essential genes have been replaced with the gene of interest. Non-cytopathic viruses include retroviruses (e.g., lentivirus), the life cycle of which involves reverse transcription of genomic viral RNA into DNA with subsequent proviral integration into host cellular DNA. Retroviruses have been approved for human gene therapy trials. Most useful are those retroviruses that are replication-deficient (i.e., capable of directing synthesis of the desired proteins, but incapable of manufacturing an infectious particle). Such genetically altered retroviral expression vectors have general utility for the high-efficiency transduction of genes in vivo. Standard protocols for producing replication-deficient retroviruses (including the steps of incorporation of exogenous genetic material into a plasmid, transfection of a packaging cell lined with plasmid, production

of recombinant retroviruses by the packaging cell line, collection of viral particles from tissue culture media, and infection of the target cells with viral particles) are provided in Kriegler, 1990 and in Murry, 1991).

Preferred viruses for certain applications are the adeno-viruses and adeno-associated viruses, which are double-stranded DNA viruses that have already been approved for human use in gene therapy. The adeno-associated virus can be engineered to be replication deficient and is capable of infecting a wide range of cell types and species. It further has advantages such as, heat and lipid solvent stability; high transduction frequencies in cells of diverse lineages, including hemopoietic cells; and lack of superinfection inhibition thus allowing multiple series of transductions. Reportedly, the adeno-associated virus can integrate into human cellular DNA in a site-specific manner, thereby minimizing the possibility of insertional mutagenesis and variability of inserted gene expression characteristic of retroviral infection. In addition, wild-type adeno-associated virus infections have been followed in tissue culture for greater than 100 passages in the absence of selective pressure, implying that the adeno-associated virus genomic integration is a relatively stable event. The adeno-associated virus can also function in an extrachromosomal fashion.

Other vectors include plasmid vectors. Plasmid vectors have been extensively described in the art and are well known to those of skill in the art. See e.g. Sambrook et al., 1989. In the last few years, plasmid vectors have been used as DNA vaccines for delivering antigen-encoding genes to cells in vivo. They are particularly advantageous for this because they do not have the same safety concerns as with many of the viral vectors. These plasmids, however, having a promoter compatible with the host cell, can express a peptide from a gene operatively encoded within the plasmid. Some commonly used plasmids include pBR322, pUC18, pUCl9, pRC/CMV, SV40, and pBlueScript. Other plasmids are well known to those of ordinary skill in the art. Additionally, plasmids may be custom designed using restriction enzymes and ligation reactions to remove and add specific fragments of DNA. Plasmids may be delivered by a variety of parenteral, mucosal and topical routes. For example, the DNA plasmid can be injected by intramuscular, eye, intradermal, subcutaneous, or other routes. It may also be administered by intranasal sprays or drops, rectal suppository and orally. It may also be administered into the epidermis or a mucosal surface using a gene-gun. The plasmids may be given in an aqueous solution, dried onto gold particles or in association with another DNA delivery system including but not limited to liposomes, dendrimers, cochleate and microencapsulation.

In a particular embodiment, the antisense oligonucleotide, siRNA, shRNA or ribozyme nucleic acid sequence is under the control of a heterologous regulatory region, e.g., a heterologous promoter. The promoter may be specific for Muller glial cells, microglia cells, endothelial cells, pericyte cells and astrocytes For example, a specific expression in Muller glial cells may be obtained through the promoter of the glutamine synthetase gene is suitable. The promoter can also be, e.g., a viral promoter, such as CMV promoter or any synthetic promoters.

In a particular embodiment, an endonuclease can be used to abolish the expression of the gene, transcript or protein variants of EZH2.

Indeed, as an alternative to more conventional approaches, such as cDNA overexpression or downregulation by RNA interference, new technologies provide the means to manipulate the genome. Indeed, natural and engineered nuclease enzymes have attracted considerable attention in the recent years. The mechanism behind endonuclease-based genome inactivating generally requires a first step of DNA single or double strand break, which can then trigger two distinct cellular mechanisms for DNA repair, which can be exploited for DNA inactivating: the error prone non homologous end-joining (NHEJ) and the high-fidelity homology-directed repair (HDR).

In a particular embodiment, the endonuclease is CRISPR-cas. As used herein, the term "CRISPR-cas" has its general meaning in the art and refers to clustered regularly interspaced short palindromic repeats associated which are the segments of prokaryotic DNA containing short repetitions of base sequences.

In some embodiment, the endonuclease is CRISPR-cas9 which is from Streptococcus pyogenes. The CRISPR/Cas9 system has been described in US 8697359 B1 and US 2014/0068797. Originally an adaptive immune system in prokaryotes (Barrangou and Marraffini, 2014), CRISPR has been recently engineered into a new powerful tool for genome editing. It has already been successfully used to target important genes in many cell lines and organisms, including human (Mali et al., 2013, Science, Vol. 339 : 823–826), bacteria (Fabre et al., 2014, PLoS Negl. Trop. Dis., Vol. 8:e2671.), zebrafish (Hwang et al., 2013, PLoS One, Vol. 8:e68708.), C. elegans (Hai et al., 2014 Cell Res. doi: 10.1038/cr.2014.11.), bacteria (Fabre et al., 2014, PLoS Negl. Trop. Dis., Vol. 8:e2671.), plants (Mali et al., 2013, Science, Vol. 339 : 823–826), Xenopus tropicalis (Guo et al., 2014, Development, Vol. 141 : 707–714.), yeast (DiCarlo et al., 2013, Nucleic Acids Res., Vol. 41 : 4336–4343.), Drosophila (Gratz et al., 2014 Genetics, doi:10.1534/genetics.113.160713), monkeys (Niu et al., 2014, Cell, Vol. 156 : 836–843.), rabbits (Yang et al., 2014, J. Mol. Cell Biol., Vol. 6 : 97-99.), pigs (Hai et al., 2014, Cell

Res. doi: 10.1038/cr.2014.11.), rats (Ma et al., 2014, Cell Res., Vol. 24 : 122–125.) and mice (Mashiko et al., 2014, Dev. Growth Differ. Vol. 56 : 122–129.). Several groups have now taken advantage of this method to introduce single point mutations (deletions or insertions) in a particular target gene, via a single gRNA. Using a pair of gRNA-directed Cas9 nucleases instead, it is also possible to induce large deletions or genomic rearrangements, such as inversions or translocations. A recent exciting development is the use of the dCas9 version of the CRISPR/Cas9 system to target protein domains for transcriptional regulation, epigenetic modification, and microscopic visualization of specific genome loci.

In some embodiment, the endonuclease is CRISPR-Cpf1 which is the more recently characterized CRISPR from Provotella and Francisella 1 (Cpf1) in Zetsche et al. ("Cpf1 is a Single RNA-guided Endonuclease of a Class 2 CRISPR-Cas System (2015); Cell; 163, 1-13).

In order to test the functionality of a putative EZH2 degrader a test is necessary. For that purpose, to identify an EZH2 degrader, we can evaluate its activity by analyzing the level of EZH2 in the cells after treatment by western blotting.

In another embodiment, the invention relates to a method for treating a resistant leukemia comprising administering to a patient in need thereof a therapeutically effective amount of an EZH2 degrader or an inhibitor of the EZH2 gene expression.

Diagnostic method

In a particular embodiment, the resistant leukemic cells of the invention have a high level of H3K27me3 at specific genes compared to non-resistant leukemic cells. Thus, level of H3K27me3 at these genes can be used as biomarker of resistant leukemia cells.

The invention also relates to a method to diagnose or predict a resistant leukemia of a subject suffering from a leukemia comprising determining, in a biological sample from the patient the level of H3K27me3.

Thus, another object of the invention relates to an in vitro method for diagnosing or predicting a resistant leukemia in a patient suffering a leukemia comprising i) determining in a sample obtained from the subject the histone methylation profile level of H3K27 ii) comparing the histone methylation profile level of H3K27 at step i) with its predetermined reference value and iii) providing a bad diagnosis or prognosis when the histone methylation profile level determined at step i) is higher than its predetermined reference value, or providing a good diagnosis or prognosis when the histone methylation profile level determined at step i) is lower than its predetermined reference value.

As used herein, the term “bad diagnosis or prognosis” denotes that the patient has a resistant leukemia.

According to the invention, the histone methylation profile level of H3K27 denotes methylation profile of H3K27 and notably the profile of H3K27 tri-methylated (H3K27m3). A patient with a high level of H3K27m3 will have a bad diagnosis or prognosis.

Methods for extracting chromatin from biological samples and determining the histone methylation level are well known in the art. Commonly, chromatin isolation procedures comprise lysis of cells after one step of crosslink that will fix proteins that are associated with DNA. After cell lysis, Chromatin is fragmented, immunoprecipitated and DNA is recovered. DNA is then extracted with phenol, precipitated in alcohol, and dissolved in an aqueous solution.

The H3K27 methylation level can be determined by chromatin IP (see for example Boukarabila H., et al, 2009) ChIP-chip or by ChIP-qPCR (see for example the materiel and methods part and Wu J. et al., 2006).

According to the invention the "reference value” is the histone methylation level of H3K27 determined in a biological sample of a subject not afflicted by a leukemia or by a resistant leukemia. Preferably, said normal level of histone methylation is assessed in a control sample (e.g., sample from a healthy patient, which is not afflicted by a resistant leukemia) and preferably, the average of histone methylation profile level in several control samples.

Therapeutic composition

Another object of the invention relates to a therapeutic composition comprising an EZH2 degrader or an inhibitor of the EZH2 gene expression according to the invention for use in the treatment of a resistant leukemia in a patient in need thereof.

In another particular embodiment, the invention relates to a therapeutic composition comprising an EZH2 degrader or an inhibitor of the EZH2 gene expression according to the invention to sensitive resistant cancerous cells to therapeutic compounds used to treat leukemia.

Any therapeutic agent of the invention may be combined with pharmaceutically acceptable excipients, and optionally sustained-release matrices, such as biodegradable polymers, to form therapeutic compositions.

"Pharmaceutically" or "pharmaceutically acceptable" refers to molecular entities and compositions that do not produce an adverse, allergic or other untoward reaction when

administered to a mammal, especially a human, as appropriate. A pharmaceutically acceptable carrier or excipient refers to a non-toxic solid, semi-solid or liquid filler, diluent, encapsulating material or formulation auxiliary of any type.

The form of the pharmaceutical compositions, the route of administration, the dosage and the regimen naturally depend upon the condition to be treated, the severity of the illness, the age, weight, and sex of the patient, etc.

The pharmaceutical compositions of the invention can be formulated for a topical, oral, intranasal, parenteral, intraocular, intravenous, intramuscular or subcutaneous administration and the like.

Preferably, the pharmaceutical compositions contain vehicles which are pharmaceutically acceptable for a formulation capable of being injected. These may be in particular isotonic, sterile, saline solutions (monosodium or disodium phosphate, sodium, potassium, calcium or magnesium chloride and the like or mixtures of such salts), or dry, especially freeze-dried compositions which upon addition, depending on the case, of sterilized water or physiological saline, permit the constitution of injectable solutions.

The doses used for the administration can be adapted as a function of various parameters, and in particular as a function of the mode of administration used, of the relevant pathology, or alternatively of the desired duration of treatment.

In addition, other pharmaceutically acceptable forms include, e.g. tablets or other solids for oral administration; time release capsules; and any other form currently can be used.

Pharmaceutical compositions of the present invention may comprise a further therapeutic active agent. The present invention also relates to a kit comprising an agonist, antagonist or inhibitor of the expression according to the invention and a further therapeutic active agent.

For example, anti-cancer agents may be added to the pharmaceutical composition as described below.

Anti-cancer agents may be Melphalan, Vincristine (Oncovin), Cyclophosphamide (Cytoxan), Etoposide (VP-16), Doxorubicin (Adriamycin), Liposomal doxorubicin (Doxil) and Bendamustine (Treanda).

Others anti-cancer agents may be for example cytarabine (AraC), anthracyclines, fludarabine, gemcitabine, capecitabine, methotrexate, taxol, taxotere, mercaptopurine, thioguanine, hydroxyurea, cyclophosphamide, ifosfamide, nitrosoureas, platinum complexes such as cisplatin, carboplatin and oxaliplatin, mitomycin, dacarbazine, procarbizine, etoposide, teniposide, campathecins, bleomycin, doxorubicin, idarubicin, daunorubicin, dactinomycin,

plicamycin, mitoxantrone, L-asparaginase, doxorubicin, epimbicm, 5-fluorouracil, taxanes such as docetaxel and paclitaxel, leucovorin, levamisole, irinotecan, estramustine, etoposide, nitrogen mustards, BCNU, nitrosoureas such as carmustme and lomustine, vinca alkaloids such as vinblastine, vincristine and vinorelbine, imatimb mesylate, hexamethyhnelamine, topotecan, kinase inhibitors, phosphatase inhibitors, ATPase inhibitors, tyrphostins, protease inhibitors, inhibitors herbimycm A, genistein, erbstatin, idrarubucin, volasertib, tozasertib (VX-680), nutlin 3, olaparib and lavendustin A. In one embodiment, additional anticancer agents may be selected from, but are not limited to, one or a combination of the following class of agents: alkylating agents, plant alkaloids, DNA topoisomerase inhibitors, anti-folates, pyrimidine analogs, purine analogs, DNA antimetabolites, taxanes, podophyllotoxin, hormonal therapies, retinoids, photosensitizers or photodynamic therapies, angiogenesis inhibitors, antimitotic agents, isoprenylation inhibitors, cell cycle inhibitors, actinomycins, bleomycins, MDR inhibitors and Ca2+ ATPase inhibitors.

Additional anti-cancer agents may be selected from, but are not limited to, cytokines, chemokines, growth factors, growth inhibitory factors, hormones, soluble receptors, decoy receptors, monoclonal or polyclonal antibodies, mono-specific, bi-specific or multi-specific antibodies, monobodies, polybodies.

Additional anti-cancer agents may be selected from, but are not limited to, growth or hematopoietic factors such as erythropoietin and thrombopoietin, and growth factor mimetics thereof.

In the present methods for treating resistant AML the further therapeutic active agent can be an antiemetic agent. Suitable antiemetic agents include, but are not limited to, metoclopromide, domperidone, prochlorperazine, promethazine, chlorpromazine, trimethobenzamide, ondansetron, granisetron, hydroxyzine, acethylleucine monoemanolamine, alizapride, azasetron, benzquinamide, bietanautine, bromopride, buclizine, clebopride, cyclizine, dunenhydrinate, diphenidol, dolasetron, meclizme, methallatal, metopimazine, nabilone, oxypemdyl, pipamazine, scopolamine, sulpiride, tetrahydrocannabinols, thiefhylperazine, thioproperazine and tropisetron. In a preferred embodiment, the antiemetic agent is granisetron or ondansetron.

In another embodiment, the further therapeutic active agent can be an hematopoietic colony stimulating factor. Suitable hematopoietic colony stimulating factors include, but are not limited to, filgrastim, sargramostim, molgramostim and epoietin alpha.

In still another embodiment, the other therapeutic active agent can be an opioid or non-opioid analgesic agent. Suitable opioid analgesic agents include, but are not limited to,

morphine, heroin, hydromorphone, hydrocodone, oxymorphone, oxycodone, metopon, apomorphine, nomioiphine, etoipbine, buprenorphine, mepeddine, lopermide, anileddine, ethoheptazine, piminidine, betaprodine, diphenoxylate, fentanil, sufentanil, alfentanil, remifentanil, levorphanol, dextromethorphan, phenazodne, pemazocine, cyclazocine, methadone, isomethadone and propoxyphene. Suitable non-opioid analgesic agents include, but are not limited to, aspirin, celecoxib, rofecoxib, diclofinac, diflusinal, etodolac, fenoprofen, flurbiprofen, ibuprofen, ketoprofen, indomethacin, ketorolac, meclofenamate, mefanamic acid, nabumetone, naproxen, piroxicam and sulindac.

In yet another embodiment, the further therapeutic active agent can be an anxiolytic agent. Suitable anxiolytic agents include, but are not limited to, buspirone, and benzodiazepines such as diazepam, lorazepam, oxazapam, chlorazepate, clonazepam, chlordiazepoxide and alprazolam.

In yet another embodiment, the further therapeutic active agent can be a checkpoint blockade cancer immunotherapy agent.

Typically, the checkpoint blockade cancer immunotherapy agent is an agent which blocks an immunosuppressive receptor expressed by activated T lymphocytes, such as cytotoxic T lymphocyte-associated protein 4 (CTLA4) and programmed cell death 1 (PDCD1, best known as PD-1), or by NK cells, like various members of the killer cell immunoglobulin-like receptor (KIR) family, or an agent which blocks the principal ligands of these receptors, such as PD-1 ligand CD274 (best known as PD-L1 or B7-H1).

Typically, the checkpoint blockade cancer immunotherapy agent is an antibody.

In some embodiments, the checkpoint blockade cancer immunotherapy agent is an antibody selected from the group consisting of anti-CTLA4 antibodies, anti-PD1 antibodies, anti-PDL1 antibodies, anti-PDL2 antibodies, anti-TIM-3 antibodies, anti-LAG3 antibodies, anti-IDO1 antibodies, anti-TIGIT antibodies, anti-B7H3 antibodies, anti-B7H4 antibodies, anti-BTLA antibodies, and anti-B7H6 antibodies.

The invention will be further illustrated by the following figures and examples. However, these examples and figures should not be interpreted in any way as limiting the scope of the present invention.

FIGURES:

Figure 1: Impact of targeting Ezh2 on APL Progression. Experimental scheme of the analysis of RA, GSK or combo treated bone marrow. (A) Cell viability of PLZF-RARA

TG cells upon GSK126 (GSK) or MS1943 (MS) treatments monitored by bioluminescence. Results are expressed by percent of living cells and normalized to the untreated condition (NT). results are expressed as the mean ±SD of three independent experiments (n=3). *p-value < 0.05, *** p-value < 0.001. (B) In vitro efficiency of MS1943 on EZH2 protein level. PLZF-RARA TG cells are treated for 96H with increasing doses of MS1943 (MS) (NT: 0, 1.25, 2.5, 5 µM). Global levels of Ezh2 and H3K27me3 detected by western blotting (WB) in each indicated condition. Actin is used as loading control. Signal intensity is measured and normalized according to the loading control and to the untreated condition. (C) Survival rate (Kaplan Meier survival analysis, https://www.statskingdom.com/kaplan-meier.html) of mice transplanted with untreated (NT), MS1943 (MS, 2.5µM) or GSK126 (GSK, 2.5µM) pretreated PLZF-RARA TG bone marrow. *** p-value < 0.001.

EXAMPLE:

Material & Methods

Cell Culture

Human U937 MT, U937 B412 (PLZF-RARA expressing cells), U937 PR9 (PML-RARA), 293T and murine Fdcp1 and 416b cell lines were maintained at exponential growth in Roswell Park Memorial Institute (RPMI) (Gibco) or Dulbecco's-modified Eagle's medium (DMEM) supplemented with 10% foetal calf serum (FCS) and 1% penicillin/streptomycin. PLZF-RARA TG BM cells were grown in Iscove's Modified Dulbecco's Medium (Gibco) containing 20% of FCS and 1% penicillin/streptomycin and supplemented with 20 ng/ml IL-6, 20 ng/ml IL-3, 50 ng/ml SCF and 10 ng/ml GM-CSF (PreproTech). PLZF-RARA and PML-RARA expression was achieved by treating U937 cell lines with 0.1 mM of ZnSO4 for at least 48 hours.

293T cells were transfected with PLZF-RARA and/or Ezh2-Flag constructs by CaCl2 coprecipitation.

For cell viability, 20,000 PLZF-RARA TG BM cells or 10,000 Fdcp1 and 416b cells were cultured for 96 hours with GSK126 or MS1943 (MedChemExpress). Cell viability was evaluated using the CellTiter-Glo® Luminescent Cell Viability Assay according to the manufacturer's instructions.

Mouse in vivo experiments

The PLZF-RARA/RARA-PLZF-induced APL mouse model (called here PLZF-RARA model) was previously described by Pandolfi and colleagues (Cheng et al., 2000). For transplantation, 0.5 millions of Cd45.2 leukemic cells were transplanted in sub-lethally

irradiated (1.5 Gy) NSG mice. APL development was monitored by standard hematological procedures and mice were sacrificed for promyelocyte purification at 2-2.5-weeks post transplantation. All-Trans Retinoic Acid (RA) (MedChemExpress) was reconstituted in 90% corn oil and 10% DMSO and was intraperitoneally administered at a dose of 0.8-1 mg per mice for 3 or 7 consecutive days. GSK126 (MedChemExpress) was reconstituted in 20% SBE-β-CD adjusted to pH 4-4.5 with 1 N acetic, supplemented with 10% DMSO, and was intraperitoneally injected at a dose of 1.25 mg per mice for 10 consecutive days.

Ezh2fl/fl mice were crossed with Rosa26::Cre-ERT mice (TaconicArtemis GmbH) to achieve the conditional deletion of Ezh2 (Mochizuki-Kashio et al., 2011). To induce Cre-ERT activity for in vivo Ezh2 deletion, these mice were intraperitoneally injected with 100 µl of tamoxifen dissolved in corn oil at a concentration of 10 mg/ml for 5 consecutive days.

APL models were bred and maintained in the CRCM mouse facility (Marseille, France) in accordance with institutional guidelines for the use of laboratory animals and approved by the French authority (authorization number: 23893) and Ezh2 models were bred and maintained in the animal research facility of the Graduate School of Medicine, Chiba University (Chiba, Japan) in accordance with institutional guidelines.

Purification of Lineage negative cells and leukemic myeloid progenitors

Tibias, femurs and hips were crushed in PBS containing 3% of fetal calf serum (FCS). Red blood cells were lysed using ACK buffer (Gibco). Lineage negative cells (Lin-) were obtained by depleting Cre-ERT-Ezh2fl/fl bone marrow in mature cells expressing the lineage markers Cd5, B220, Cd11b, Gr-1, Ter-119, 7-4 using the lineage cell depletion kit (Miltenyi Biotec). Leukemic bone marrow was purified by depleting Cd4, Cd8a, B220, Cd11c, Cd3e, Ter-119, Dx5 and in Cd45.1 using biotin antibodies. Leukemic myeloid progenitors (Promyelocytes: Cd45.2+, C-Kit+, Gr1+; ProReP : Cd45.2+, C-Kit+, Gr1+ , Cd48+, Cd11b- ; NeuRA : Cd45.2+, C-Kit+, Gr1+ , Cd48-, Cd11b+) were purified using the FACS Aria III cell sorter (Beckman Dickinson).

Viral production and transduction of Lineage negative cells

To produce the recombinant retroviruses, pMy-IRES-PLZF-RARA-GFP plasmid or the pMy-IRES-GFP empty vector were transfected into PlatE packaging cells by CaCl2 coprecipitation. Before transduction, Lin- cells were pre-cultured for 24 hours in S-Clone SF-03 (Sanko Junyaku) with 0.2 % BSA (Stemcell technologies), 1% penicillin/streptomycin, 50µM β-mercapto ethanol and supplemented with 20 ng/ml IL-6, 20 ng/ml IL-3, 50 ng/ml SCF and 10 ng/ml GM-CSF (PreproTech). Cells were then spinoculated with retroviral supernatant

in the presence of protamine sulfate (10 mg/mL; Sigma-Aldrich) for 30 minutes at 1350g and 32°C. 48 hours later, GFP positive cells were sorted on FACS Aria III cell sorter.

Colony assays

GFP positive cells (PLZF-RARA or IRES transduced Lin- cells) were cultured 48 hours in the same S-Clone SF-03 complete medium than described above and 1 x 104 cells were seeded into M3234 methylcellulose (Stemcell technologies). Cells were replated every 1-2 weeks. For Ezh2 deletion (data not shown), 150nM 4-OHT was directly added into the methylcellulose medium. For the experiment described in Figure 1, 2.5 µM of GSK126 and/or 1 µM of RA were added into the methylcellulose. At each replating, cells were cytospun and their morphology was analyzed by May-Grünwald staining. Immunophenotypic analysis (C-Kit, Cd11b, Gr, FceR1, Cd45.2) were performed by FACS.

Protein extraction, Co-Immunoprecipitations and Western Blotting (WB)

For co-immunoprecipitation (Co-IP) in U937 or 293T cells, nuclear proteins were extracted using the dounce homogenizer with high salt concentration according to Dignam and Roeder. https://www.ncbi.nlm.nih.gov/pubmed/20150077. 100 µg of nuclear extracts were diluted in isotonic buffer, precleared with Protein A or G agarose beads (Thermo Scientific) and incubated overnight at 4°C with Rabbit IgG (Cell Signaling Technology), EZH2 (Active Motif), SUZ12 (Active Motif), FLAG (Sigma Aldrich) or PLZF 2A9 (Active Motif) antibodies. Protein A or G agarose beads were added the next day for 2 hours and the resulting complexes were washed, denatured and eluted in the Laemmli sample buffer.

For WB in promyelocytes or CFU-cells, cells were directly lysed in the Laemmli sample buffer. Proteins were separated on SDS-PAGE. Proteins were blotted on nitrocellulose membranes and incubated with different primary antibodies: PLZF 2A9 (Active Motif) and D9 clones (Santacruz), EZH2 (BD Biosciences), H3K27me3 (Active Motif). ACTIN (Sigma Aldrich) and/or H3 (Active Motif) were used as loading control. Proteins were revealed using a peroxidase conjugated secondary antibody and ECLTM Prime or Select Western Blotting Detection Reagent (Amersham).

Reverse-Transcription and PCR quantitative (RT-qPCR)

Total RNA was extracted using the RNeasy Plus Micro kit (Qiagen). cDNA was synthesized with the Transcriptor High Fidelity cDNA Synthesis Kit (Roche). Real-time PCR was performed using the SsoADV Univer SYBR Green Supermix (Bio-Rad) and detected with a CFX96 RealTime PCR Detection System (Bio-Rad). Relative expression levels were determined by the $2^{\wedge-\Delta CT}$ method using Actb as housekeeping gene.

Chromatin immunoprecipitation-sequencing (ChIP-seq)

Three to 5 millions of purified promyelocytes were fixed with 1% of formaldehyde for 8 min. Reaction was quenched by adding 2 mM of glycine. Fixed pellets were washed twice with cold PBS and lysed with Lysis Buffer A (0.25% Triton X100, 10 mM Tris-HCl pH8, 10 mM EDTA, 0.5 mM EGTA), and Lysis Buffer B (250 mM NaCl, 50 mM Tris-HCl pH8, 1 mM EDTA, 0.5 mM EGTA). Nuclei were suspended in Buffer C (0.5% SDS, 10 mM Tris-HCl pH8, 1mM EDTA, 0.5 mM EGTA) and chromatin was sonicated using the Bioruptor® Pico (Diagenode) in order to obtain DNA fragments with an average size of 300 bp. After centrifugation, the soluble chromatin was diluted in Buffer D (0.6% Triton X100, 0.06% NaDOC, 150 mM NaCl, 12 mM Tris-HCl pH8, 1 mM EDTA, 0.5 mM EGTA) and immunoprecipitated overnight at 4°C with magnetic beads (Active Motif) pre-incubated with the following antibodies: H3K27me3 (Cell Signalling), H3K27ac (Active Motif), H3K4me1 (Abcam), H3K4me3 (Diagenode). A, B, C, D buffers were supplemented with 1X protease inhibitor cocktail (PIC) (Life Technology # 11873580001) and 0.5 mM PMSF. ChIP were washed with the following combinations of wash buffers: W1 (1% Triton X100, 0.1% NaDOC, 150 mM NaCl, 10 mM Tris-HCL pH8), W2 (0.5% NP40, 0.5% Triton X100, 0.5% NaDOC, 150 mM NaCl, 10 mM Tris-HCL pH8), W3 (0.7% Triton X100, 0.1% NaDOC, 250 mM NaCl, 10 mM Tris-HCL pH8), W4 (0.5% NP40, 0.5% NaDOC, 250 mM LiCl, 20mM Tris-HCL pH8, 1mM EDTA, W5 (0.1% NP40, 150 mM NaCl, 20 mM Tris-HCL pH8, 1 mM EDTA), W6 (20 mM Tris-HCL pH8, 1 mM EDTA). Immunoprecipitated DNA was purified with I-Pure Kit (Diagenode). ChIP-seq libraries were generated using the MicroPlex Library Preparation Kit (Diagenode) following the manufacturer's instructions and analyzed on a 2100 Bioanalyzer system (Agilent) prior sequencing. Sequencing was performed with a Next-seq500 sequencer (Illumina) using a 75-nt single-end protocol, at the Paoli Calmettes Institute Sequencing Facility (IPC, Marseille).

Analysis of ChIP-seq data

Sequencing quality control was determined using the FastQC tool (http://www.bioinformatics.babraham.ac.uk/projects/fastqc/). Reads with a Phred quality score less than 30 were filtered out.

Reads were mapped to an "hybrid genome" combining Mus musculus (GRCm38/mm10) and Drosophila melanogaster (dm6) genomes using default parameters of Bowtie2 (v2.3.4.1) (Langmead and Salzberg, 2012). Next, tags were sorted according to their genome of origin (mm10 or dm6). Duplicate tags were removed by samtools rmdup function and mapped tags were filtered using samtools view -F 4 for further analysis. A scaling factor

was calculated using dm6 mapped tags (H2Av-bound regions) as previously described (Egan et al., 2016) and mm10 mapped tags were normalized according to this scaling factor (Spike-in correction). Normalized-mapped reads were converted into BigWig using the deepTools suite (v2.2.4) (Ramirez et al., 2016) / bamCoverage -bs 20 --scaleFactor, multiBigwigSummary. Fragment length prediction was performed using MACS2 predictd and later applied for peak calling High confidence binding sites were determined using MACS2 callpeak broad mode / --broad-cutoff 0.05 -q 0.01 --extsize. Inputs were used as controls. Bedtools intersect (v2.17.0) (Quinlan and Hall, 2010) with a minimum overlap of 1-base was used to determine enhancer coordinates. To map H3K27ac and H3K27me3 signals on enhancer coordinates we applied computeMatrix (v3.5.0) from the deepTools suite / --afterRegionStartLength --beforeRegionStartLength --referencePoint = center --skipZeros.

All sequencing data were visualized using the Integrative Genomics Viewer (IGV v2.3.92) (Robinson et al., 2011). Biological functions associated with poised enhancers were determined using Genomic Regions Enrichment of Annotations Tool (data not shown) (GREAT v3.0.0) (McLean et al., 2010) or ClusterProfiler package (data not shown). The GREAT tool was also used for assigning enhancers to the closest genes.

scRNA-seq library preparation and sequencing

FACS purified promyelocytes were loaded 30 min after the sorting onto a Chromium Single Cell Chip and processed with the Chromium Controller (10x Genomics) according to the manufacturer's instructions for single cell barcoding at a target capture rate of 6000 individual cells per sample. Libraries were prepared using Chromium Single-Cell 3′ Reagent Kits v2 (10x Genomics). Sequencing was performed with a Next-seq500 sequencer (Illumina) using a 75-nt single-end protocol, at the Paoli Calmettes Institute Sequencing Facility (IPC, Marseille).

Upstream analysis of scRNA-seq data

scRNA-seq processing was performed following the 10X Genomics workflow (https://support.10xgenomics.com/single-cell-gene-expression/software/overview/welcome) using the 10X software CellRanger (v4.0). The demultiplexing was done with cellranger mkfastq (Illumina bcl2fastq wrapper). Next we used cellranger count to generate single cell feature count with mm10 as reference genome. We recovered 5,786 Ctrl and 7,416 RA cells with 3,667 Ctrl and 3,396 RA median genes per cell.

Downstream analysis of scRNA-seq data

In this section, we only report the parameter settings we have modified. All other parameters were set to default. All the downstream analyses were performed using the Seurat

(v4.0.0) package (Hao et al., 2021) unless explicitly specified. The following pipeline was applied. (1) A QC step for both samples / subset function (count number using Median Absolute Deviation (MAD) and the fraction of mitochondrial genes); 5,106 Ctrl and 6,794 RA d7 cells were obtained. (2) Exclusion of genes expressed in less than 0.001 * number of cells (5.1 Ctrl and 6.7 RA d7 cells) / CreateSeuratObject function, min.cells parameter. (3) Cell cycle phase prediction using the cyclone package (training dataset of synchronized mouse embryonic stem cells); G0 was grouped with G1 phase. (4) Data normalization / NormalizeData function with scaling factor 10,000 log. (5) Detection of the 2,000 most highly variable genes (HVG) / FindVariableFeatures function, selection.method = "vst". (6) Integration anchors between both batches were calculated using the HVG and a Canonical Correlation Analysis (CCA) / FindIntegrationAnchors function, dims = 1:15. (7) These integration anchors were used to integrate both samples / IntegrateData function, dims = 1:15. (8) Integrated dataset were scaled and the cell cycle effect was regressed / ScaleData function, vars.to.regress equal to G2_M, S, G1_G0. (9) PCA was performed on the scaled dataset / RunPCA function, npcs = 50. (10) Uniform Manifold Approximation and Projection (UMAP) was calculated using PCA component / RunUMAP function, dims = 1:15. (11) A K-nearest neighbor graph was constructed and used to cluster the cells with Louvain algorithm / FindNeighbors function, dims = 1:15; FindClusters function, resolution = 0.3. The 6 obtained clusters were manually annotated using Differentially Expressed Genes (DEG) and gene list enrichments. DEGs were computed for each cluster in order to identify cluster markers by using the FindAllMarkers (Wilcoxon rank sum tests on the log-normalized data of the given cluster against all the other) (Table S1); only genes expressed in at least 10% of cells in either of the two groups and with a log fold change threshold of 0.25 were tested / min.pct = 0.1; logfc.threshold = 0.25. An adjusted p-value (Bonferroni correction) with a threshold of 0.05 was applied to filter out non-significant markers. Markers for the RA d7 condition were calculated using the FindMarkers function for each cluster using the same parameters as cluster markers / ident.1 = RA 7d, ident.2 = Ctrl.

To further characterize the identified clusters, we performed gene set enrichment analysis on the cluster markers using g:Profiler package (v0.7.0) / custom_bg = all genes in the dataset. GO term (GO:BP, GO:MF, GO:CC), KEGG, REACT, TF, MI, CORUM, HP, HPA and OMIM database enrichments were tested (data not shown).

The expression of Senescence Associated Secretory Phenotype (SASP) Reactome (https://www.gsea-msigdb.org/gsea/msigdb/cards/REACTOME_SENESCENCE_ASSOCIATED_SECRETOR

Y_PHENOTYPE_SASP) and "Enhancer switch" (data not shown) signatures were tested in the dataset; expression scores were calculated for each individual cell using the AddModuleScore function. These signatures were tested between clusters and between cluster conditions using FindAllMarkers / min.pct = 0, logfc.threshold = 0, p_val_adj < 0.05.

Trajectory analysis of scRNA-seq data

Pseudotime ordering and trajectory were performed using Single-cell Trajectories Reconstruction, Exploration And Mapping (STREAM, v1.0) (Chen et al., 2019). The classical STREAM pipeline was applied. (1) Selection of the top principal components on all genes / select_top_principal_components, n_pc=15; first_pc=True. (2) Dimension reduction / dimension_reduction, method=mlle; feature=top_pcs, n_components=4, n_neighbors=50. (3) Trajectory inference / seed_elastic_principal_graph, n_clusters=10. (4) Learning elastic principal graph / elastic_principal_graph, epg_alpha=0.01; epg_mu=0.05; epg_lambda=0.05. (5) Extension of the elastic principal graph / extend_elastic_principal_graph, epg_ext_mode=WeigthedCentroid; epg_extext_par=0.8. The resulting trajectory and pseudotime were visualized on the UMAP.

scATAC-seq library preparation and sequencing

Nuclei from FACS purified promyelocytes were purified according 10x Genomics instructions and processed using the Chromium Next GEM Single Cell ATAC Reagent Kits v1.1 and Single Index Kit N Set A according to the manufacturer's instructions for single cell barcoding at a target capture rate of 10,000 nuclei per sample. Sequencing was performed with a HiSeq2500 sequencer (Illumina) using a 150 nt paired-end protocol (Read 1N: 50 cycles, i7 Index: 8 cycles, i5 Index : 16 cycles, Read 2N: 50 cycles), at the Institute of Medical Science, Tokyo University.

Upstream and Downstream analysis of scATAC-seq data

scATAC-seq processing was performed following the cellranger-atac (v1.2.0) software from 10X Genomics. To demultiplex and generate the fastq files cellranger-atac mkfastq and then cellranger-atac count were used with mm10 genome as reference. After these steps, a total of 4,723 Ctrl and 6,418 RA cells with respectively 18,226 and 14,466 median fragments per cell was conserved. The downstream analysis was done using Seurat (v4.0.0) (Hao et al., 2021) and Signac (v1.1.1) (Stuart et al., 2020). The following pipeline was applied. (1) QC step (number of fragments, fraction of reads in peaks, blacklist region, nucleosome signal and TSS enrichment); 4,215 Ctrl cells and 5,806 RA d7 cells were identified. (2) LSI dimensionality reduction / Signac RunTFIDF function, FindTopFeatures function setting min.cutoff=q75 and

RunSVD function on the peaks assay with n= 40. (3) Gene expression matrix scoring by assigning each peak to the nearest gene (– 2 kb) / Signac GeneActivity function.

Integration of scRNA-seq and scATAC-seq data

For each scATAC-seq sample we performed the following steps. In the first step we performed cluster imputation from the scRNA-seq annotated clusters. We applied the Seurat function FinTransferAnchors on the CCA to capture the shared feature correlation structure between the scRNA-seq and the scATAC-seq / query assay equal to the ATAC gene activity, reference equal to a subset of scRNA-seq cells according to the condition (Ctrl or RA d7), features equal to the 2000 scRNA-seq HVG. The cell identity of scATAC-seq cells was assigned using Seurat TransferData using the calculated anchors / refdata equal to the six scRNA-seq clusters, dims= 2:30, weight.reduction= LSI. Cells with the prediction score lower than 40% were discarded; 3,954 Ctrl cells and 3,413 RA d7 cells were conserved. In a second step we performed RNA imputation of the 2000 HVG from the scRNA-seq. We applied the Seurat function FindTransferAnchors on the CCA and imputed the expression of the 2000 HVG by using Seurat TransferData and the newly identified anchors / query assay equal to the ATAC gene activity, reference equal all scRNA-seq cells, features equal to the 2000 RNA HVG; refdata equal to the 2000 HVG expression matrix, dims=2:30, weight.reduction=LSI. Both scATAC-seq samples were merged together; next, merged scATAC-seq were merged with the scRNA-seq data. HVG of the resulting merged object was scaled using Seurat ScaleData / features equal to the HVG, do.scale=FALSE. PCA dimensionality reduction was performed using Seurat RunPCA (features equal to the HVG). UMAP was calculated using PCA components / Seurat RunUMAP function, dims = 1:15.

Transcription factor motif accessibility and regulon prediction

TF activities were calculated on the merged annotated scATAC-seq using RunChromVAR function from the Signac implementation of chromVAR (Schep et al., 2017) (Stuart et al., 2020) and the human JASPAR 2020 database (Fornes et al., 2020) (633 TFS) / genome = BSgenome.Mmusculus.UCSC.mm10. The resulting motif activity matrix was used to identify differential activity scores between clusters / Seurat FindAllMarkers, test.use=LR; latent.vars=nCount_peaks. TF regulons were found using pySCENIC (1.10.0) (Aibar et al., 2017). The raw expression matrix of integrated Ctrl and RA d7 scRNA-seq datasets was filtered by keeping genes expressed in more than 2% of total cells; 10,777 genes passed the filtering. In order to obtain a more robust outcome we ran 50 iterations of pySCENIC / grn, grnboost method, and different fixed seeds [run 1 : --seed 1, run n : --seed n]. TFs were identified using the SCENIC motif database (motifs-v9-nr.mgi-m0.001-o0.0) and TF targets using cis Target

database (mm9-tss-centered-10kb-7species.mc9nr). Different subsets of data (Ctrl only, RA d7 only, Ctrl and RA d7 together) were used to run the analysis. Each iteration was refined by excluding targets with no TF motif enrichment / pyscenic ctx, --mask_dropouts. We recovered the positive and negative regulons /option -a. Two steps of filtering were then applied: (1) only the regulons and the genes identified as TF targets in 80% of the runs were conserved. The AUCell function of pySCENIC was run on these consensus regulons.

APL patient analyses

A total of 9 APL patient (3 PLZF-RARA; 6 PML-RARA) affymetrix RNA microarrays were analyzed (GSM211183, GSM211184, GSM211185, GSM1057933, GSM1057934, GSM1057935, GSM1057936, GSM1057937, GSM1057938). Each group was processed separately using the following steps. Briefly, CEL files were read using ReadAffy function from affy package (v1.66.0) and normalization steps (background adjustment, log transformation) were carried out using gcrma package (v2.60.0). Probes were annotated using annotationDbi (v1.50.0) and hgu133a2.db (v3.2.3) packages, and probes from the same transcript were merged and median value was kept. PLZF-RARA and PML-RARA groups were then merged together and potential batch effects were removed using quantile normalization. Finally, DEG analysis was performed using linear model fit and Empirical Bayes statistics from the limma package (v3.44.1). For gene set enrichment analyses (GSEA) we used the ReP and NeuRA gene markers and two computed signatures. The “Methyl. targeting” signature consisted of a list of differentially expressed genes in GSK-treated versus untreated cells. The “Non methyl. targeting” signature was obtained by subtracted the previous gene list to the list of differentially expressed genes in MS1943-treated versus untreated cells.

Results

Single-cell transcriptome analysis reveals a subset of retinoic acid resistant leukemic cells with DNA repair and proliferation signatures

To decipher mechanisms linked to APL t(11;17) relapse and identify features of RA-resistant leukemic cells, we used droplet-based single-cell RNA sequencing (scRNA-seq) on the 10X Genomics platform for the PLZF-RARA leukemic cells obtained from bone marrow of PLZF-RARA-TG transplanted mice (Cheng et al., 2000) at day 17 post transplantation, treated or not with RA (data not shown). Effect of the RA-treatment was monitored by following increased expression of cell surface markers (Cd11b and Gr1) and by morphology analyses of FACS-sorted promyelocytes (data not shown). After filtering, quality control, and doublet exclusion, we obtained the transcriptome of 5106 untreated (Ctrl) and 6794 RA-treated

(d7) promyelocytes, which were then corrected to reduce batch and cell cycle effects and integrated using the Seurat workflow (Stuart et al., 2019) (data not shown). Dimensionality reduction and unsupervised clustering, done using uniform manifold approximation and projection (UMAP) (McInnes et al., 2018), in all cells (treated and untreated), identified six clusters that were annotated by enrichment analysis of their gene markers. Five of the clusters had neutrophil associated signatures (Prom1, Prom2, Prom3, NeuRA1, NeuRA2) consistent with the promyelocytic stage of induced leukemia, while one cluster was characterized by genes involved in DNA replication associated with DNA repair and proliferation processes (ReP) (data not shown C). Prom1, Prom2 and Prom3 were enriched with untreated cells suggesting their fading upon RA treatment (data not shown), while NeuRA1 and NeuRA2 appeared almost exclusively in RA-treated cells. Both clusters strongly expressed myeloid differentiation genes such as Cd177 and Ly6g (encoding neutrophil surface markers) or such as Lcn2 (encoding a neutrophil gelatinase-associated lipocalin precursor), but low level of the stem/progenitor surface marker Cd34 (data not shown). They also showed high expression of myeloid transcription factors (TFs) such as Cebpd, Gfi1, Spi1 and Retnlg, as well as reduced expression of the myeloid repressor Ikzf2, suggesting their terminal myeloid differentiated state. By contrast the ReP cluster was characterized by the expression of genes involved in homologous recombination and cell-cycle such as Pcna, Mcm3 and Rad51 (data not shown) and was equally composed of Ctrl and RA-treated cells (data not shown) suggesting that RA treatment did not impact on the cell identity of these promyelocytes.

To determine the potential differentiation journey of the RA-treated transformed promyelocytes, we ordered on pseudotime Ctrl and RA-treated cells based on their transcriptional similarities with the Single-cell Trajectories Reconstruction, Exploration And Mapping (STREAM) pipeline (Chen et al., 2019) (data not shown). STREAM analysis revealed three trajectories split into five different states of promyelocytes (segments A, B, C, D, E), (data not shown). Integration of STREAM ordering and UMAP partitioning allow us to define the departure of the trajectories at the extremity of state A, which was mostly composed of ReP cells. Trajectories 1 (states A-C-D) and 2 (states A-C-E) ended towards RA differentiated cells, since their final states C, D and E were largely composed RA-treated cells grouped in NeuRA1 and NeuRA2, respectively (data not shown), confirming a pronounced differentiating effect of RA on a portion of PLZF-RARA expressing cells and consistent with a stronger expression of differentiation marker in NeuRA2 (data not shown). Interestingly, the third trajectory (state B), which went far into the pseudotime was composed mostly of Ctrl cells grouped in Prom2 and Prom3 (data not shown), suggesting a spontaneous differentiation program in leukemic cells.

This analysis showed a pronounced but partial differentiating effect of RA on PLZF-RARA expressing cells and designated cells in the ReP cluster as the treatment-persistent cells.

To further investigate the RA (un)responsiveness of the identified clusters, we took advantage of available transcriptional signatures reflecting RA sensitivity of PML-RARA versus RA resistant PLZF-RARA murine APL (Ablain et al., 2014). We found that the NeuRA1 and NeuRA2 clusters were enriched with a computed PML-RARA RA-responsive signature (see Mat & Med) confirming that the two clusters were composed of RA-responsive blasts (data not shown). By contrast, the ReP cluster was highly enriched with the proliferative E2F signature (data not shown), which persisted upon RA treatment (data not shown), likely supporting the malignancy and RA insensitivity of these cells. Besides, we found that the ReP cluster, unlike the Prom2, Prom3 and NeuRA1 clusters, lacked the Secretory Associated Signature Phenotype (SASP) (Reactome; GSEA), suggesting the absence of a senescence program in this cluster (data not shown). Interestingly, the ReP cluster specifically expressed the deubiquitinase Usp37 involved in PLZF-RARA fusion stability (Yang and Shih, 2013) and this expression was not impacted by the RA treatment (data not shown). To confirm the presence of the oncogenic fusion protein in this cluster after RA treatment, we attempted to purify it based on the expression of specific surface markers identified in our scRNA-seq dataset. Taking into account the expression of the resolving cell surface markers Cd48 and Itgam (Cd11b), we were limited to isolate Prom1-3 and ReP (ProReP) cells from NeuRA1 and NeuRA2 (NeuRA) cells after RA treatment. (data not shown). We found that, whereas the PLZF-RARA fusion was neither detected in the bulk nor in NeuRA populations, ProReP cells did maintain PLZF-RARA expression after RA treatment (data not shown).

Altogether, these results both reveal transcriptional heterogeneity and differentiation states within the PLZF-RARA transformed cells, which may impact on the RA response and identify the ReP cluster, which exhibits no differentiation features, high E2F signature and PLZF-RARA residual expression, as the potential driver of RA resistance of PLZF-RARA leukemia.

Integrative single-cell multi-omics analysis highlights chromatin genes as potential actors of RA resistance of PLZF-RARA expressing cells

To characterize at the regulatory/epigenomic level the heterogeneity underlying PLZF-RARA transformation and RA response at the regulatory/epigenomic level, we took advantage of the single cell epigenomic (scATAC-seq) technology and generated a chromatin accessibility profile of 4,215 RA-treated cells and 5,806 untreated cells in our PLZF-RARA TG mouse

model. To link transcriptome variation with changes in epigenome and to better define cell identity and function, we chose to map cells from our scATAC-seq data to the six scRNA-seq defined clusters by applying a method that detects pairwise correspondences, termed ''anchors'', between cells in two different datasets and allows their transposition into the shared space (Stuart et al., 2019). We successfully transferred scRNA-seq annotations onto scATAC-seq data of control and RA-treated promyelocytes and defined a new shared space (data not shown). Comparing the frequencies of the six clusters (defined with scRNA-seq only) in scATAC-seq and scRNA-seq datasets in the new space showed an overall good concordance between the two levels of information, emphasizing the link between chromatin structure and transcription (data not shown). This concordance was especially high on RA-treated promyelocytes (data not shown), confirming the known effect of RA on differentiation through remodeling of chromatin landscape (Gudas, 2013). In the scATAC-seq dataset the Prom1 state was detected neither in untreated nor in RA-treated cells suggesting a transitional state. Consistent with our scRNA-seq data, the ratio of scATAC-seq cells in the ReP cluster was not affected by RA treatment (7% in both conditions). The low impact of RA on chromatin opening in the ReP cluster in comparison to other clusters was confirmed by Coverage Plot visualization at some selected genes (data not shown). Thus, our analysis of scATAC-seq supports the important role of chromatin in RA activity and confirms the little impact of RA on the ReP cluster at both RNA and chromatin levels, which may drive RA resistance of PLZF-RARA cells.

Beyond cell identity, scRNA-seq and scATAC-seq data are uniquely valuable to define gene regulatory networks at the cellular scale. To decipher specific TF activity that might be associated with RA resistance, we inferred information from ATAC-seq and RNA-seq data in the ReP cells (data not shown). We first selected ReP TF activity by considering, in our scATAC-seq data, the accessibility of DNA motifs of TFs in the ReP cluster using the Signac chromVAR package (Stuart et al., 2020) (data not shown). Selected ReP TFs were cross-referenced with master transcriptional regulators identified from scRNA-seq data using Single-Cell Regulatory Network Inference and Clustering (SCENIC), which measures TF regulon activity (Aibar et al., 2017) (data not shown). Doing so and in line with our previous annotation, we identified 3 TFs, linked to E2F (E2F1, E2F4, TFDP1) with high transcriptional activity in the ReP cluster (data not shown). Interestingly E2f1 and Tfdp1 regulon activity were increased upon RA treatment while E2f4 activity was diminished (data not shown). Next, we focused on their 176 shared targets and looked at both the accessibility at gene promoters (±3 kb from the transcriptional start site [TSS]) and distal regulatory regions (enhancers) as well as at the

expression levels of the target genes in the ReP cluster (data not shown). K-means clustering taking into account the three levels of information highlighted five clusters of genes (data not shown), which could account for the heterogeneity in gene regulation inside the regulons. We observed that for most of the heatmap clusters, the average ATAC signal appeared stronger at enhancer regions than at promoters. Yet, we evidenced a dynamic in chromatin and transcriptional events starting with high chromatin opening and low RNA expression (Cl_1 and Cl_2) and ending with high RNA expression and low chromatin opening (Cl_5), in agreement with a previous observation that cis-regulatory regions were often opened prior to any gene expression (Ranzoni et al., 2021). This means a sequential coordination for a given TF to regulate its targets. Two clusters of genes (Cl_4 and Cl_5) were highly expressed in comparison to the others and were specifically not impacted by RA treatment in the ReP cells in comparison to the NeuRA2 cells, composing a RA unresponsive cluster (data not shown). In line with our previous analysis, these highly expressed genes (Pcna, Mcm2-7 and Ezh2) were related to DNA repair, proliferation and chromatin (data not shown).

The results show that RA transcriptional resistance can be defined at the chromatin level and is dependent on E2F transcriptional activity and chromatin accessibility differences mainly at enhancer regions of the genome of a subset of promyelocytes. We also pointed out heterogeneity in terms of target regulation inside of a regulon.

EZH2 is necessary for PLZF-RARA transformation activity

Because EZH2 is frequently involved in AML, we focused on this chromatin remodeler enzyme, a component of the polycomb group protein 2 (PRC2) whose canonical activity is involved in the deposition of the repressive histone mark H3K27me3 (Lund et al., 2014). To ascertain the functional relevance of Ezh2 in PLZF-RARA APL cells, we first confirmed its high expression in the ReP cluster and the persistence of its expression after RA-treatment (data not shown). We also confirmed the chromatin accessibility in its promoter region at the E2F1, E2F4 and TFDP1 binding motifs (data not shown). Next, we analyzed the clonogenic activity of PLZF-RARA in the absence of EZH2 ex vivo by transducing BM lineage negative cells of a conditional KO Ezh2 mouse model (Mochizuki-Kashio et al., 2011) with a PLZF-RARA-IRES-GFP retroviral construct and performing replating assay (data not shown). Consistent with our single cell data, PLZF-RARA transduction in lineage-negative cells induced an overall increase in both EZH2 and H3K27me3 levels (data not shown) while sustaining repeated replatings (data not shown). Ezh2 deletion (Δ/Δ) induced by adding 4-OHT into the methylcellulose, even in the absence of RA, reduced the cell number and dramatically altered

the replating capacity of the PLZF-RARA expressing cells (data not shown) and promoted their terminal differentiation (data not shown). Ezh2 deletion and the consecutive H3K27me3 loss were associated with a PLZF-RARA decrease (data not shown) which was consistent with the altered replating capacity and differentiation status of the cells. This loss in replating capacity was also observed when Ezh2 deletion was achieved in vivo before PLZF-RARA transduction (data not shown) or ex vivo after the transformation process at the second or third round of plating (data not shown). Ezh2 deletion at these steps of replating decreased the proliferation of cells and prevented them to form colonies at the next round of replating (data not shown). These assays suggest that Ezh2 is required for the initiation and maintenance of PLZF-RARA clonogenic activity.

We next investigated a potential interaction between the oncogenic fusion protein PLZF-RARA and EZH2 using a myeloid cell line (U937-B412) with zinc inducible PLZF/RARA expression and HEK293T cells overexpressing a Flag-tagged EZH2 and PLZF-RARA. In both systems, we could not demonstrate an interaction between PLZF-RARA and EZH2 or SUZ12, another component of PRC2 (data not shown). However, when probing our SUZ12 IP with an anti-EZH2 antibody, we evidenced a stronger interaction between EZH2 and SUZ12 in the presence of PLZF-RARA than without (data not shown). The specificity of the stabilizing effect of PLZF-RARA on the EZH2/SUZ12 complex was further confirmed by showing that PML-RARA expression did not have this effect (data not shown).

Collectively, these results reveal a dependency of PLZF-RARA expressing leukemic cells upon EZH2 whose activity may itself be modified by the presence of the fusion protein.

PLZF-RARA modulates chromatin landscape and EZH2 methyltransferase activity at pro-apoptotic genes

To further define the relationship between EZH2 and PLZF-RARA, we studied EZH2 chromatin activity in relation to PLZF-RARA expression. We compared the epigenetic landscape of PLZF-RARA promyelocytes with the Granulocyte-Monocyte-Progenitor (GMP) compartment, which is the closest cell compartment to promyelocytes according to its transcriptional signature (data not shown) and is therefore the most appropriate normal counterpart of PLZF-RARA promyelocytes. Because our scATAC-seq data revealed stronger chromatin opening at enhancer regions than promoters (data not shown) and cis-regulatory enhancer elements are known to influence the development of leukemia (Bhagwat et al., 2018), we mapped the four histone marks (H3K27ac, H3K27me3, H3K4me1 and H3K4me3) that allow to discriminate active (H3K27ac-enriched) and poised (H3K27me3-enriched) enhancers

(Poplineau et al., 2019) (data not shown). By comparing PLZF-RARA promyelocytes with GMP genomic enhancer distribution, we found that PLZF-RARA expression significantly modified poised (H3K27me3-enriched) enhancer positions (68% of them were specific to PLZF-RARA condition) while minimally affecting the active enhancers (70 % of them were overlapping in the two conditions) (data not shown). These new putative H3K27me3-enriched enhancer regions in PLZF-RARA condition reflected a shift in H3K27me3 enrichment from enhancers regulating developmental processes to those regulating kinase signaling and bloodstream systems (data not shown). Next, we wondered whether this gain of H3K27me3 occurred at sites marked by H3K27ac in GMP condition, which would be then considered as an enhancer "switch" or at new genomic loci considered as "de novo enhancers" data not shown). Among poised enhancers found only in the PLZF-RARA condition, 3701 appeared at new genomic loci whereas 175 were active in GMP condition, suggesting that the main effect of PLZF-RARA is to promote de novo enhancers. However, when we queried the expression of enhancer-related genes in our scRNA-seq dataset, we found that the switched enhancers exerted a specific effect on the ReP cluster since the expression of nearby genes were lower in this cluster in comparison to the others (data not shown). In contrast, de novo enhancer-associated genes were equally weakly expressed in all scRNA-seq clusters (data not shown). Altogether, this suggests that this specific ReP enhancer switch might be linked to RA unresponsiveness. Gene Ontology (GO) analysis revealed that genes related to the switched enhancers were associated with myeloid cell differentiation and with pro-apoptotic program regulation terms (data not shown). Among the genes pertinent for differentiation and leukemia we found Bin1, P2rx4, Dusp6 and Ly86 that presented an H3K27ac/H3K27me3 enhancer switch (data not shown). Consistently, the expression of these genes was lower in the presence of PLZF-RARA than in GMPs (data not shown).

Altogether, these data suggest that PLZF-RARA expression led to a redistribution of repressed enhancers and thus restraining apoptosis and myeloid differentiation and suggesting an important role of histone methyltransferase activity in PLZF-RARA APL transformation.

<u>High H3K27me3 level at enhancers of pro-apoptotic genes marks RA-induced relapse initiating cells</u>

To determine the chromatin function of EZH2 in RA resistance, we monitored EZH2 chromatin activity at relapse after RA treatment (data not shown). As previously observed (Ablain et al., 2014), RA treatment, although inducing a clear differentiation of blasts (data not shown), did not eradicate relapse-initiating cells, since relapse was observed at day 17 post-

transplant in mice transplanted with RA-treated BMs (data not shown). In accordance with our scRNA-seq data that showed a global increase in Ezh2 mRNA in RA-treated PLZF-RARA cells (data not shown), we observed as early as d3 a higher level of EZH2 protein in the RA treated BM than in the untreated BM (data not shown). This higher level was conserved after the secondary transplantation of treated BM (td3 and td7) (data not shown). Importantly, the overall level of H3K27me3 did not follow the level of EZH2 in RA-treated BM, suggesting a contrasting effect of RA on EZH2: an increase of its level but an inhibition of its histone methyltransferase activity, while leukemia relapse was characterized with a restoration of high levels of H3K27me3 level in the BM (data not shown). Interestingly, H3K27me3 signal at poised enhancers was decreased resulting in a diminution in numbers of these enhancers after 3 or 7 days of RA treatment (data not shown). Yet, leukemia relapse was characterized with a restoration of high levels of H3K27me3 level at enhancers and a high number of H3K27me3 (data not shown). These results show that differentiation of PLZF-RARA promyelocytes is accompanied by a partial loss of H3K27me3 but not of EZH2 and that relapsed-leukemia is characterized by high levels of both H3K27me3 and EZH2.

Because we suspected that the switched enhancers that mark the ReP cluster retained H3K27me3 and could support RA resistance, we measured the levels of H3K27me3/H3K27ac after RA treatment and at relapse in the 175 switched enhancers (data not shown). We found that neither RA treatment (3 or 7 days) nor the following transplantations erased the H3K27me3 signal at these enhancers in ReP cells, for which H3K27ac stayed lower than in GMP (data not shown). Consistently, the signature of the switched enhancers was not impacted by RA in our scRNA-seq data (data not shown). Thus, RA, despite inducing a global loss in H3K27me3 level and differentiation, did not affect H3K27me3 at some specific loci. In addition, our results pointed out a divergence between EZH2 protein level and its methyltransferase activity.

Altogether, these results suggest that high H3K27me3 level at enhancers of pro apoptotic genes is a marker of RA resistance.

Targeting EZH2 to eradicate relapse initiating cells

Because EZH2 is necessary for PLZF-RARA induced transformation and high H3K27me3 level at specific loci is a marker of resistance, we questioned the pertinence of targeting EZH2 with GSK126 in combination with RA to overcome resistance.

To test this hypothesis, we treated PLZF-RARA TG transplanted mice with the GSK126 drug for 3 days followed by 7 consecutive days of RA and transplanted the treated BMs into new recipients to follow disease progression according to the pre-treatment (data not shown).

At first, the inhibitory effect of GSK on H3K27me3 level in the treated BM, which was more pronounced when the drug was administered in combination with RA, was confirmed by western blot (data not shown). However, GSK treatment did not affect the % of PLZF-RARA TG cells as reflected by the % of Cd45.2 positive cells in total BM nor, in contrast to RA, impacted on disease progression and blast differentiation (data not shown). Besides, no synergistic effect of GSK with RA was observed (data not shown). Leukemia relapse was monitored by following the transplantation of the treated BMs in new recipient mice (data not shown). At day 13 post transplantation, GSK treated BM expanded as untreated BM suggesting that GSK alone did not impact the relapse initiating cells. A delay in leukemia progression was observed in the RA-treated BM, but addition of the GSK did not change in any instance the leukemia progression.

To rule out accessibility and dosage problems that could be faced using animal models, we compared the effect of GSK treatment alone or in combination with RA on PLZF-RARA replating capacity (data not shown). As for the in vivo experiment, GSK alone or in combination with RA had no effect on the replating capacity of PLZF-RARA ex vivo (data not show). However, as revealed by morphological and FACS analyses, PLZF-RARA transduced cells exhibited some differentiated cell features upon GSK that were more pronounced upon RA or RA plus GSK treatments, evidenced by the presence of granules into their cytoplasm and loss of the KIT stem-progenitor marker (after exclusion of Kit+, FcεR1+ mast cells) (data not shown). These data showed that despite a strong dependency of PLZF-RARA cell transformation and a RA response on EZH2 activity, inhibition of its catalytic activity is not sufficient to promote APL clearance and further suggested that PLZF-RARA APL depends on a non-canonical activity of EZH2. To explore this possibility, we took advantage of a new commercially available EZH2 degrader, MS1943 (Ma et al., 2020). PLZF-RARA TG BM was treated with MS and re-transplanted in new recipient mice (data not shown). We observed a strong effect of the MS on cell viability (Figure 1A) concomitant to its ability to erase H3K27me3 level and efficiently degraded EZH2 (Figure 1B), which was higher in PLZF-RARA cells than in cells that did not express the fusion (data not shown). Reinjecting alive MS-treated PLZF-RARA BM cells in recipient mice significantly prolonged the survival of the mice, confirming the importance of EZH2 non-canonical activity in PLZF-RARA transformation (Figure 1C). To link this loss of leukemic potential upon EZH2 degradation to a transcriptional reprogramming, we performed bulk RNA-seq on PLZF-RARA TG BM treated with MS or GSK (data not shown). MS treatment was associated with a more pronounced and specific decrease in the expression of ReP cluster marker genes in comparison to GSK treatment

(data not shown). Gene ontology analysis on genes modified by MS further confirmed the importance to degrade EZH2 to target the biological processes (cell cycle and DNA-dependent DNA replication) associated with RA resistance (data not shown). Interestingly, the gene signature resulting from the targeting of methyltransferase activity of EZH2 (named methyl. targeting) as well as the ReP marker genes were positively correlated to PLZF-RARA patients while genes associated with the targeting of EZH2 non-methyltransferase activity (named Non methyl. targeting) and the NeuRA marker genes were correlated to PML-RARA patients (data not shown). These data not only show that our RA (un)-response signatures identified in our mouse model could be used for APL patients; they also confirm that targeting EZH2 non-methyltransferase activities is necessary to promote RA sensitivity in APL patients.

CONCLUSION

All together this result demonstrates that targeting EZH2 methyltransferase activity is not sufficient to eradicate relapse leukemia initiating cells and suggest that PLZF-RARA leukemia depends upon catalytic and non-catalytic activity of EZH2.

REFERENCES:

Throughout this application, various references describe the state of the art to which this invention pertains. The disclosures of these references are hereby incorporated by reference into the present disclosure.

Ablain, J., Rice, K., Soilihi, H., de Reynies, A., Minucci, S., and de The, H. (2014). Activation of a promyelocytic leukemia-tumor protein 53 axis underlies acute promyelocytic leukemia cure. Nat Med 20, 167-174. 10.1038/nm.3441.

Aibar, S., Gonzalez-Blas, C.B., Moerman, T., Huynh-Thu, V.A., Imrichova, H., Hulselmans, G., Rambow, F., Marine, J.C., Geurts, P., Aerts, J., et al. (2017). SCENIC: single-cell regulatory network inference and clustering. Nat Methods 14, 1083-1086. 10.1038/nmeth.4463.

Arteaga, M.F., Mikesch, J.H., Qiu, J., Christensen, J., Helin, K., Kogan, S.C., Dong, S., and So, C.W. (2013). The histone demethylase PHF8 governs retinoic acid response in acute promyelocytic leukemia. Cancer Cell 23, 376-389. 10.1016/j.ccr.2013.02.014.

Bhagwat, A.S., Lu, B., and Vakoc, C.R. (2018). Enhancer dysfunction in leukemia. Blood 131, 1795-1804. 10.1182/blood-2017-11-737379.

Brien, G.L., Stegmaier, K., and Armstrong, S.A. (2019). Targeting chromatin complexes in fusion protein-driven malignancies. Nat Rev Cancer 19, 255-269. 10.1038/s41568-019-0132-x.

Basheer, F., Giotopoulos, G., Meduri, E., Yun, H., Mazan, M., Sasca, D., Gallipoli, P., Marando, L., Gozdecka, M., Asby, R., et al. (2019). Contrasting requirements during disease evolution identify EZH2 as a therapeutic target in AML. J Exp Med 216, 966-981. 10.1084/jem.20181276.

Boukarabila, H., Saurin, A.J., Batsche, E., Mossadegh, N., van Lohuizen, M., Otte, A.P., Pradel, J., Muchardt, C., Sieweke, M., and Duprez, E. (2009). The PRC1 Polycomb group complex interacts with PLZF/RARA to mediate leukemic transformation. Genes Dev 23, 1195-1206. 23/10/1195 [pii]

10.1101/gad.512009.

Brien, G.L., Stegmaier, K., and Armstrong, S.A. (2019). Targeting chromatin complexes in fusion protein-driven malignancies. Nat Rev Cancer 19, 255-269. 10.1038/s41568-019-0132-x.

Bullinger, L., Dohner, K., and Dohner, H. (2017). Genomics of Acute Myeloid Leukemia Diagnosis and Pathways. J Clin Oncol 35, 934-946. 10.1200/JCO.2016.71.2208.

Bushweller, J.H. (2019). Targeting transcription factors in cancer - from undruggable to reality. Nat Rev Cancer 19, 611-624. 10.1038/s41568-019-0196-7.

Chen, H., Albergante, L., Hsu, J.Y., Lareau, C.A., Lo Bosco, G., Guan, J., Zhou, S., Gorban, A.N., Bauer, D.E., Aryee, M.J., et al. (2019). Single-cell trajectories reconstruction, exploration and mapping of omics data with STREAM. Nature Communications 10, 1903. 10.1038/s41467-019-09670-4.

Cheng, T., Rodrigues, N., Shen, H., Yang, Y., Dombkowski, D., Sykes, M., and Scadden, D.T. (2000). Hematopoietic stem cell quiescence maintained by p21cip1/waf1. Science 287, 1804-1808. 10.1126/science.287.5459.1804.

de The, H., and Chen, Z. (2010). Acute promyelocytic leukaemia: novel insights into the mechanisms of cure. Nat Rev Cancer 10, 775-783. 10.1038/nrc2943.

de The, H., Pandolfi, P.P., and Chen, Z. (2017). Acute Promyelocytic Leukemia: A Paradigm for Oncoprotein-Targeted Cure. Cancer Cell 32, 552-560. 10.1016/j.ccell.2017.10.002.

Di Croce, L. (2005). Chromatin modifying activity of leukaemia associated fusion proteins. Hum Mol Genet 14 Spec No 1, R77-84. 10.1093/hmg/ddi109.

Dos Santos, G.A., Kats, L., and Pandolfi, P.P. (2013). Synergy against PML-RARa: targeting transcription, proteolysis, differentiation, and self-renewal in acute promyelocytic leukemia. J Exp Med 210, 2793-2802. 10.1084/jem.20131121.

Duan, R., Du, W., and Guo, W. (2020). EZH2: a novel target for cancer treatment. Journal of Hematology & Oncology 13, 104. 10.1186/s13045-020-00937-8.

Egan, B., Yuan, C.C., Craske, M.L., Labhart, P., Guler, G.D., Arnott, D., Maile, T.M., Busby, J., Henry, C., Kelly, T.K., et al. (2016). An Alternative Approach to ChIP-Seq Normalization Enables Detection of Genome-Wide Changes in Histone H3 Lysine 27 Trimethylation upon EZH2 Inhibition. PLoS One 11, e0166438. 10.1371/journal.pone.0166438.

Folk, W.P., Kumari, A., Iwasaki, T., Pyndiah, S., Johnson, J.C., Cassimere, E.K., Abdulovic-Cui, A.L., and Sakamuro, D. (2019). Loss of the tumor suppressor BIN1 enables ATM Ser/Thr kinase activation by the nuclear protein E2F1 and renders cancer cells resistant to cisplatin. J Biol Chem 294, 5700-5719. 10.1074/jbc.RA118.005699.

Fornes, O., Castro-Mondragon, J.A., Khan, A., van der Lee, R., Zhang, X., Richmond, P.A., Modi, B.P., Correard, S., Gheorghe, M., Baranasic, D., et al. (2020). JASPAR 2020: update of the open-access database of transcription factor binding profiles. Nucleic Acids Res 48, D87-D92. 10.1093/nar/gkz1001.

Geoffroy, M.C., Esnault, C., and de The, H. (2021). Retinoids in hematology: a timely revival? Blood 137, 2429-2437. 10.1182/blood.2020010100.

Grignani, F., De Matteis, S., Nervi, C., Tomassoni, L., Gelmetti, V., Cioce, M., Fanelli, M., Ruthardt, M., Ferrara, F.F., Zamir, I., et al. (1998). Fusion proteins of the retinoic acid receptor-alpha recruit histone deacetylase in promyelocytic leukaemia. Nature 391, 815-818.

Grignani, F., Ferrucci, P.F., Testa, U., Talamo, G., Fagioli, M., Alcalay, M., Mencarelli, A., Grignani, F., Peschle, C., Nicoletti, I., and et al. (1993). The acute promyelocytic leukemia-specific PML-RAR alpha fusion protein inhibits differentiation and promotes survival of myeloid precursor cells. Cell 74, 423-431. 10.1016/0092-8674(93)80044-f.

Gudas, L.J. (2013). Retinoids induce stem cell differentiation via epigenetic changes. Semin Cell Dev Biol 24, 701-705. 10.1016/j.semcdb.2013.08.002.

Hao, Y., Hao, S., Andersen-Nissen, E., Mauck, W.M., 3rd, Zheng, S., Butler, A., Lee, M.J., Wilk, A.J., Darby, C., Zager, M., et al. (2021). Integrated analysis of multimodal single-cell data. Cell 184, 3573-3587 e3529. 10.1016/j.cell.2021.04.048.

He, L.Z., Guidez, F., Tribioli, C., Peruzzi, D., Ruthardt, M., Zelent, A., and Pandolfi, P.P. (1998). Distinct interactions of PML-RARalpha and PLZF-RARalpha with co- repressors determine differential responses to RA in APL. Nat Genet 18, 126-135.

Holohan, C., Van Schaeybroeck, S., Longley, D.B., and Johnston, P.G. (2013). Cancer drug resistance: an evolving paradigm. Nat Rev Cancer 13, 714-726. 10.1038/nrc3599.

Hou, H.A., and Tien, H.F. (2016). Mutations in epigenetic modifiers in acute myeloid leukemia and their clinical utility. Expert Rev Hematol 9, 447-469. 10.1586/17474086.2016.1144469.

Huang, M.E., Ye, Y.C., Chen, S.R., Chai, J.R., Lu, J.X., Zhoa, L., Gu, L.J., and Wang, Z.Y. (1988). Use of all-trans retinoic acid in the treatment of acute promyelocytic leukemia. Blood 72, 567-572.

Jimenez, J.J., Chale, R.S., Abad, A.C., and Schally, A.V. (2020). Acute promyelocytic leukemia (APL): a review of the literature. Oncotarget 11, 992-1003. 10.18632/oncotarget.27513.

Kahl, M., Brioli, A., Bens, M., Perner, F., Kresinsky, A., Schnetzke, U., Hinze, A., Sbirkov, Y., Stengel, S., Simonetti, G., et al. (2019). The acetyltransferase GCN5 maintains ATRA-resistance in non-APL AML. Leukemia 33, 2628-2639. 10.1038/s41375-019-0581-y.

Kent, L.N., and Leone, G. (2019). The broken cycle: E2F dysfunction in cancer. Nature Reviews Cancer 19, 326-338. 10.1038/s41568-019-0143-7.

Kim, K.H., Kim, W., Howard, T.P., Vazquez, F., Tsherniak, A., Wu, J.N., Wang, W., Haswell, J.R., Walensky, L.D., Hahn, W.C., et al. (2015). SWI/SNF-mutant cancers depend on catalytic and non-catalytic activity of EZH2. Nat Med 21, 1491-1496. 10.1038/nm.3968.

Kent, L.N., and Leone, G. (2019). The broken cycle: E2F dysfunction in cancer. Nature Reviews Cancer 19, 326-338. 10.1038/s41568-019-0143-7.

Koubi, M., Poplineau, M., Vernerey, J., N'Guyen, L., Tiberi, G., Garciaz, S., El-Kaoutari, A., Maqbool, M.A., Andrau, J.C., Guillouf, C., et al. (2018). Regulation of the positive transcriptional effect of PLZF through a non-canonical EZH2 activity. Nucleic Acids Res 46, 3339-3350. 10.1093/nar/gky080.

Ladikou, E.E., Sivaloganathan, H., Pepper, A., and Chevassut, T. (2020). Acute Myeloid Leukaemia in Its Niche: the Bone Marrow Microenvironment in Acute Myeloid Leukaemia. Curr Oncol Rep 22, 27. 10.1007/s11912-020-0885-0.

Langmead, B., and Salzberg, S.L. (2012). Fast gapped-read alignment with Bowtie 2. Nat Methods 9, 357-359. 10.1038/nmeth.1923.

Lee, S.T., Li, Z., Wu, Z., Aau, M., Guan, P., Karuturi, R.K., Liou, Y.C., and Yu, Q. (2011). Context-specific regulation of NF-kappaB target gene expression by EZH2 in breast cancers. Mol Cell 43, 798-810. 10.1016/j.molcel.2011.08.011.

Liao, Y., Smyth, G.K., and Shi, W. (2013). The Subread aligner: fast, accurate and scalable read mapping by seed-and-vote. Nucleic Acids Res 41, e108. 10.1093/nar/gkt214.

Liao, Y., Smyth, G.K., and Shi, W. (2014). featureCounts: an efficient general purpose program for assigning sequence reads to genomic features. Bioinformatics 30, 923-930. 10.1093/bioinformatics/btt656.

Liu, Z., Hu, X., Wang, Q., Wu, X., Zhang, Q., Wei, W., Su, X., He, H., Zhou, S., Hu, R., et al. (2021). Design and Synthesis of EZH2-Based PROTACs to Degrade the PRC2 Complex for Targeting the Noncatalytic Activity of EZH2. J Med Chem 64, 2829-2848. 10.1021/acs.jmedchem.0c02234.

Lund, K., Adams, P.D., and Copland, M. (2014). EZH2 in normal and malignant hematopoiesis. Leukemia 28, 44-49. 10.1038/leu.2013.288.

Ma, A., Stratikopoulos, E., Park, K.-S., Wei, J., Martin, T.C., Yang, X., Schwarz, M., Leshchenko, V., Rialdi, A., Dale, B., et al. (2020). Discovery of a first-in-class EZH2 selective degrader. Nature Chemical Biology 16, 214-222. 10.1038/s41589-019-0421-4.

McCabe, M.T., Ott, H.M., Ganji, G., Korenchuk, S., Thompson, C., Van Aller, G.S., Liu, Y., Graves, A.P., Della Pietra, A., 3rd, Diaz, E., et al. (2012). EZH2 inhibition as a therapeutic strategy for lymphoma with EZH2-activating mutations. Nature 492, 108-112. 10.1038/nature11606.

McInnes, L., Healy, J., and Melville, J. (2018). UMAP: uniform manifold approximation and projection for dimension reduction.

McLean, C.Y., Bristor, D., Hiller, M., Clarke, S.L., Schaar, B.T., Lowe, C.B., Wenger, A.M., and Bejerano, G. (2010). GREAT improves functional interpretation of cis-regulatory regions. Nat Biotechnol 28, 495-501. 10.1038/nbt.1630.

Meers, M.P., Bryson, T.D., Henikoff, J.G., and Henikoff, S. (2019). Improved CUT&RUN chromatin profiling tools. Elife 8. 10.7554/eLife.46314.

Mochizuki-Kashio, M., Mishima, Y., Miyagi, S., Negishi, M., Saraya, A., Konuma, T., Shinga, J., Koseki, H., and Iwama, A. (2011). Dependency on the polycomb gene Ezh2 distinguishes fetal from adult hematopoietic stem cells. Blood 118, 6553-6561. 10.1182/blood-2011-03-340554.

Nasr, R., Guillemin, M.C., Ferhi, O., Soilihi, H., Peres, L., Berthier, C., Rousselot, P., Robledo-Sarmiento, M., Lallemand-Breitenbach, V., Gourmel, B., et al. (2008). Eradication of

acute promyelocytic leukemia-initiating cells through PML-RARA degradation. Nat Med 14, 1333-1342. 10.1038/nm.1891.

Noguera, N.I., Catalano, G., Banella, C., Divona, M., Faraoni, I., Ottone, T., Arcese, W., and Voso, M.T. (2019). Acute Promyelocytic Leukemia: Update on the Mechanisms of Leukemogenesis, Resistance and on Innovative Treatment Strategies. Cancers (Basel) 11. 10.3390/cancers11101591.

Papaemmanuil, E., Gerstung, M., Bullinger, L., Gaidzik, V.I., Paschka, P., Roberts, N.D., Potter, N.E., Heuser, M., Thol, F., Bolli, N., et al. (2016). Genomic Classification and Prognosis in Acute Myeloid Leukemia. N Engl J Med 374, 2209-2221. 10.1056/NEJMoa1516192.

Poplineau, M., Vernerey, J., Platet, N., N'Guyen, L., Herault, L., Esposito, M., Saurin, A.J., Guilouf, C., Iwama, A., and Duprez, E. (2019). PLZF limits enhancer activity during hematopoietic progenitor aging. Nucleic Acids Res 47, 4509-4520. 10.1093/nar/gkz174.

Quinlan, A.R., and Hall, I.M. (2010). BEDTools: a flexible suite of utilities for comparing genomic features. Bioinformatics 26, 841-842. 10.1093/bioinformatics/btq033.

Ramirez, F., Ryan, D.P., Gruning, B., Bhardwaj, V., Kilpert, F., Richter, A.S., Heyne, S., Dundar, F., and Manke, T. (2016). deepTools2: a next generation web server for deep-sequencing data analysis. Nucleic Acids Res 44, W160-165. 10.1093/nar/gkw257.

Ranzoni, A.M., Tangherloni, A., Berest, I., Riva, S.G., Myers, B., Strzelecka, P.M., Xu, J., Panada, E., Mohorianu, I., Zaugg, J.B., and Cvejic, A. (2021). Integrative Single-Cell RNA-Seq and ATAC-Seq Analysis of Human Developmental Hematopoiesis. Cell Stem Cell 28, 472-487 e477. 10.1016/j.stem.2020.11.015.

Rego, E.M., He, L.Z., Warrell, R.P., Jr., Wang, Z.G., and Pandolfi, P.P. (2000). Retinoic acid (RA) and As2O3 treatment in transgenic models of acute promyelocytic leukemia (APL) unravel the distinct nature of the leukemogenic process induced by the PML-RARalpha and PLZF-RARalpha oncoproteins. Proc Natl Acad Sci U S A 97, 10173-10178.

Reimand, J., Arak, T., Adler, P., Kolberg, L., Reisberg, S., Peterson, H., and Vilo, J. (2016). g:Profiler-a web server for functional interpretation of gene lists (2016 update). Nucleic Acids Res 44, W83-89. 10.1093/nar/gkw199.

Rishi, L., Hannon, M., Salome, M., Hasemann, M., Frank, A.K., Campos, J., Timoney, J., O'Connor, C., Cahill, M.R., Porse, B., and Keeshan, K. (2014). Regulation of Trib2 by an E2F1-C/EBPalpha feedback loop in AML cell proliferation. Blood 123, 2389-2400. 10.1182/blood-2013-07-511683.

Robinson, J.T., Thorvaldsdottir, H., Winckler, W., Guttman, M., Lander, E.S., Getz, G., and Mesirov, J.P. (2011). Integrative genomics viewer. Nat Biotechnol 29, 24-26. 10.1038/nbt.1754.

Schenk, T., Chen, W.C., Gollner, S., Howell, L., Jin, L., Hebestreit, K., Klein, H.U., Popescu, A.C., Burnett, A., Mills, K., et al. (2012). Inhibition of the LSD1 (KDM1A) demethylase reactivates the all-trans-retinoic acid differentiation pathway in acute myeloid leukemia. Nat Med 18, 605-611. 10.1038/nm.2661.

Schep, A.N., Wu, B., Buenrostro, J.D., and Greenleaf, W.J. (2017). chromVAR: inferring transcription-factor-associated accessibility from single-cell epigenomic data. Nat Methods 14, 975-978. 10.1038/nmeth.4401.

Sobas, M., Talarn-Forcadell, M.C., Martinez-Cuadron, D., Escoda, L., Garcia-Perez, M.J., Mariz, J., Mela-Osorio, M.J., Fernandez, I., Alonso-Dominguez, J.M., Cornago-Navascues, J., et al. (2020). PLZF-RARalpha, NPM1-RARalpha, and Other Acute Promyelocytic Leukemia Variants: The PETHEMA Registry Experience and Systematic Literature Review. Cancers (Basel) 12. 10.3390/cancers12051313.

Stetson, L.C., Balasubramanian, D., Ribeiro, S.P., Stefan, T., Gupta, K., Xu, X., Fourati, S., Roe, A., Jackson, Z., Schauner, R., et al. (2021). Single cell RNA sequencing of AML initiating cells reveals RNA-based evolution during disease progression. Leukemia. 10.1038/s41375-021-01338-7.

Stuart, T., Butler, A., Hoffman, P., Hafemeister, C., Papalexi, E., Mauck, W.M., 3rd, Hao, Y., Stoeckius, M., Smibert, P., and Satija, R. (2019). Comprehensive Integration of Single-Cell Data. Cell 177, 1888-1902 e1821. 10.1016/j.cell.2019.05.031.

Stuart, T., Srivastarva, A., Lareau, C., and Satija, R. (2020). Multimodal single-cell chromatin analysis with Signac. bioRxiv. https://doi.org/10.1101/2020.11.09.373613

Tallman, M.S. (2004). Acute promyelocytic leukemia as a paradigm for targeted therapy. Semin Hematol 41, 27-32. 10.1053/j.seminhematol.2004.02.004.

Tanaka, S., Miyagi, S., Sashida, G., Chiba, T., Yuan, J., Mochizuki-Kashio, M., Suzuki, Y., Sugano, S., Nakaseko, C., Yokote, K., et al. (2012). Ezh2 augments leukemogenicity by reinforcing differentiation blockage in acute myeloid leukemia. Blood 120, 1107-1117. 10.1182/blood-2011-11-394932.

Van Galen, P., Hovestadt, V., Wadsworth Ii, M.H., Hughes, T.K., Griffin, G.K., Battaglia, S., Verga, J.A., Stephansky, J., Pastika, T.J., Lombardi Story, J., et al. (2019). Single-Cell RNA-Seq Reveals AML Hierarchies Relevant to Disease Progression and Immunity. Cell 176, 1265-1281 e1224. 10.1016/j.cell.2019.01.031.

Wu, Z.L., Zheng, S.S., Li, Z.M., Qiao, Y.Y., Aau, M.Y., and Yu, Q. (2010). Polycomb protein EZH2 regulates E2F1-dependent apoptosis through epigenetically modulating Bim expression. Cell Death Differ 17, 801-810. 10.1038/cdd.2009.162.

Yang, W.C., and Shih, H.M. (2013). The deubiquitinating enzyme USP37 regulates the oncogenic fusion protein PLZF/RARA stability. Oncogene 32, 5167-5175. 10.1038/onc.2012.537.

CLAIMS:

1. An EZH2 degrader or an inhibitor of the EZH2 gene expression for use in the treatment of resistant leukemia in a patient in need thereof.

2. An EZH2 degrader for use in the treatment of resistant leukemia in a patient in need thereof.

3. The EZH2 degrader or the inhibitor of the EZH2 gene expression according to the claim 1 or 2 to sensitive resistant leukemia cancerous cells to therapeutic compounds used to treat leukemia.

4. An i) EZH2 degrader or an inhibitor of the EZH2 gene expression and a ii) therapeutic compound already used to treat leukemia as a combined preparation for simultaneous, separate or sequential use in the treatment of resistant leukemia.

5. The EZH2 degrader or the inhibitor of the EZH2 gene expression for use according to claims 1 to 4 wherein the resistant leukemia is an acute lymphocytic leukemia (ALL) or an acute myeloid leukemia (AML).

6. The EZH2 degrader or the inhibitor of the EZH2 gene expression for use according to claim 5 wherein the resistant leukemia is a resistant acute promyelocytic leukemia (APL), a resistant PLZF-RARA acute promyelocytic leukaemia (APL), a resistant cytogenetically normal AML (CN-AML), a resistant acute myeloid leukemia with trisomy 8 or a resistant acute leukemia with MLL translocations.

7. The EZH2 degrader or the inhibitor of the EZH2 gene expression for use according to claim 6 wherein the resistant leukemia is a resistant acute promyelocytic leukemia (APL) in a patient in need thereof.

8. The EZH2 degrader for use according to the claims 1 to 7 wherein the EZH2 degrader is the molecule MS1943.

9. A method for treating a resistant leukemia comprising administering to a patient in need thereof a therapeutically effective amount of an EZH2 degrader or an inhibitor of the EZH2 gene expression.

10. A method to diagnose or predict a resistant leukemia of a subject suffering from a leukemia comprising determining, in a biological sample from the patient the level of H3K27me3.

11. A therapeutic composition comprising an EZH2 degrader or an inhibitor of the EZH2 gene expression according to claim 1 for use in the treatment of a resistant leukemia in a patient in need thereof.

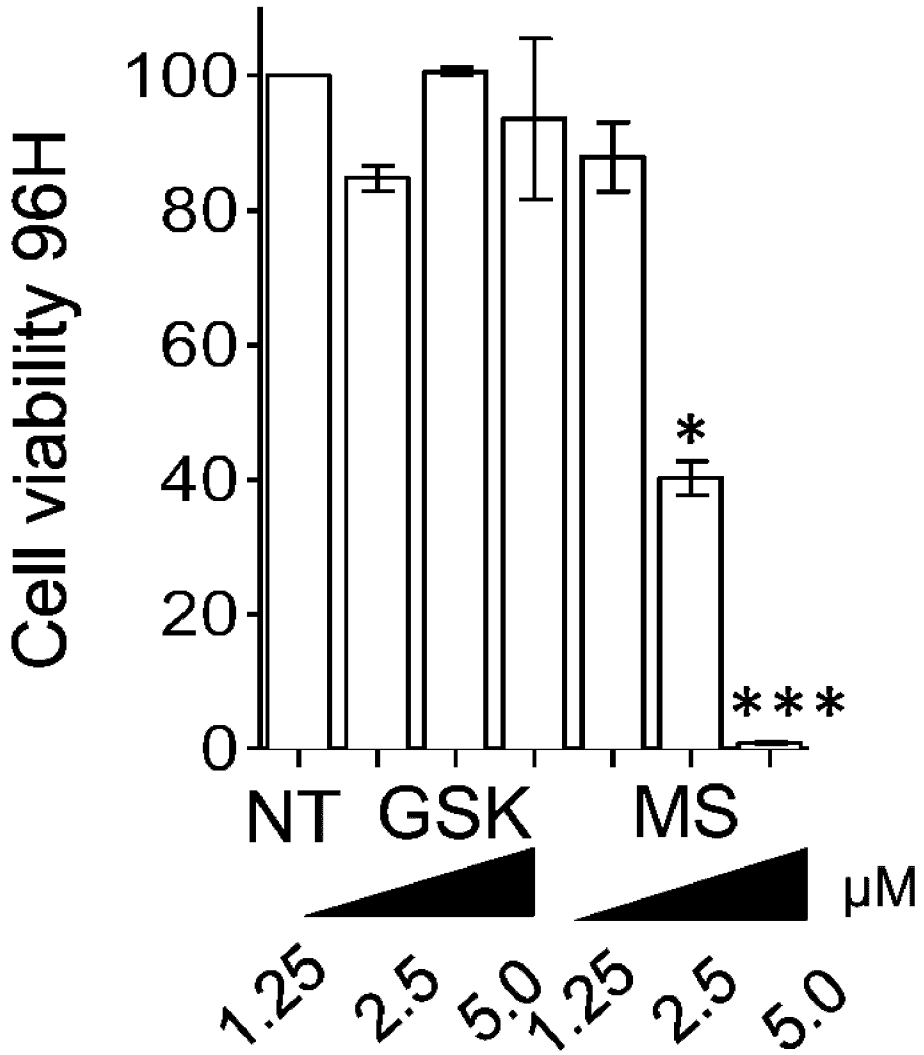
Cell viability 96H
100
80
60
40
20
0
*
***
NT
GSK
MS
µM
1.25
2.5
5.0
1.25
2.5
5.0

Figure 1A

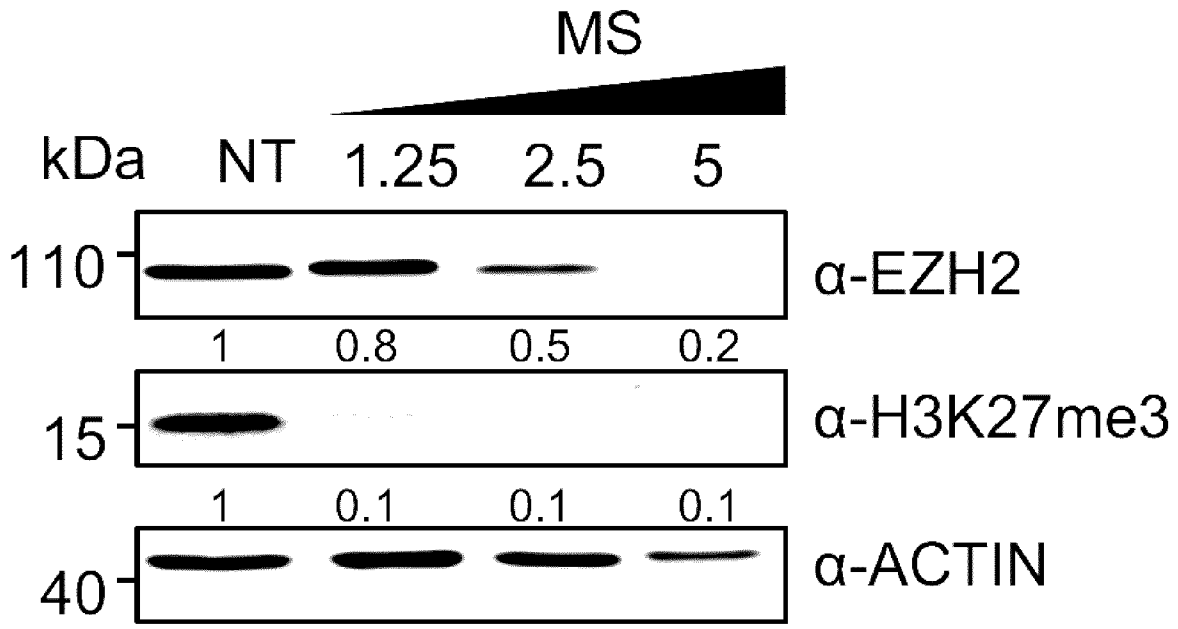

Figure 1B

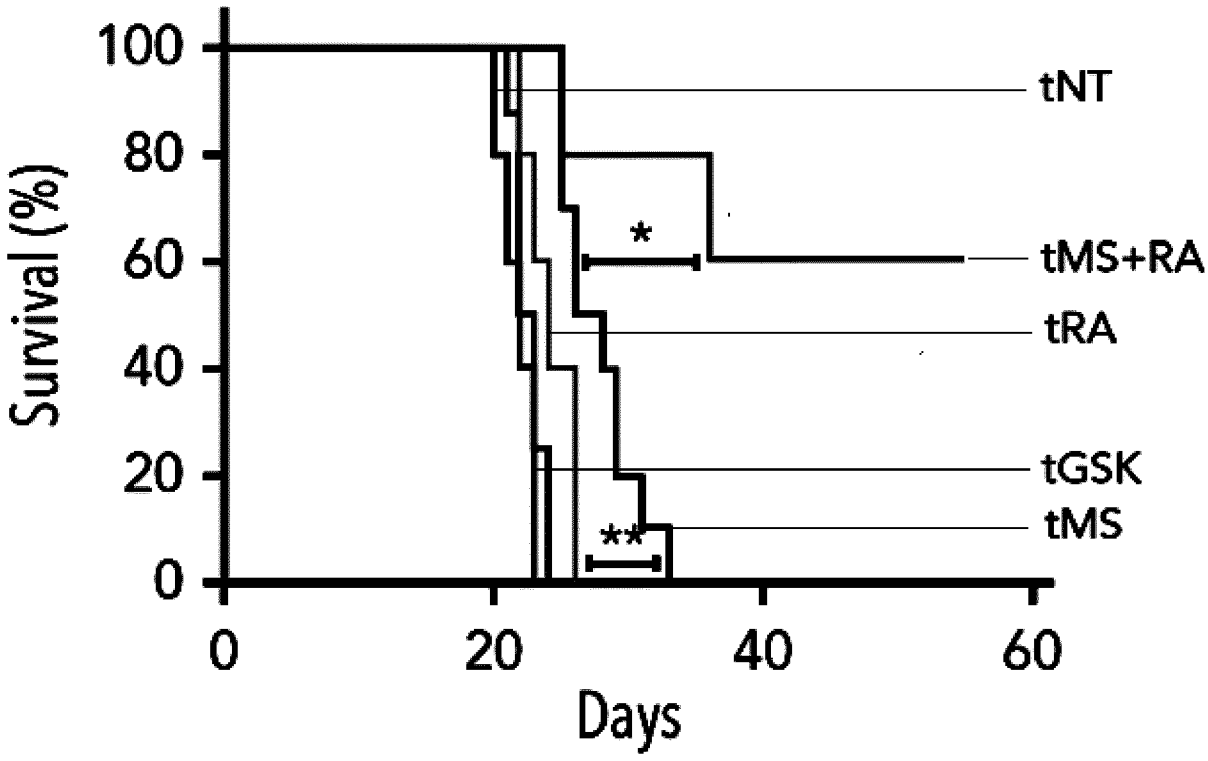

Figure 1C

INTERNATIONAL SEARCH REPORT

International application No
PCT/EP2022/086142

A. CLASSIFICATION OF SUBJECT MATTER
INV. A61K31/4155 A61K31/496 A61K45/06 A61K9/00 A61P35/02
ADD.

According to International Patent Classification (IPC) or to both national classification and IPC

B. FIELDS SEARCHED

Minimum documentation searched (classification system followed by classification symbols)
A61K A61P

Documentation searched other than minimum documentation to the extent that such documents are included in the fields searched

Electronic data base consulted during the international search (name of data base and, where practicable, search terms used)
EPO-Internal, BIOSIS, CHEM ABS Data, EMBASE, WPI Data

C. DOCUMENTS CONSIDERED TO BE RELEVANT

Category*	Citation of document, with indication, where appropriate, of the relevant passages	Relevant to claim No.
X	WO 2021/025148 A1 (DAIICHI SANKYO CO LTD [JP]) 11 February 2021 (2021-02-11)	1-7,9,11
Y	claims 1, 3, 4, 6, 7, 9, 10, 12 paragraphs [0030], [0036], [0041]	8
X	WO 2017/198870 A1 (EPI-C S R L [IT]) 23 November 2017 (2017-11-23) claims 13, 7-8 claims 9, 10 page 38, line 6 - page 39, line 2	1-3,6,7, 9-11

-/--

[x] Further documents are listed in the continuation of Box C.

[x] See patent family annex.

* Special categories of cited documents :

"A" document defining the general state of the art which is not considered to be of particular relevance

"E" earlier application or patent but published on or after the international filing date

"L" document which may throw doubts on priority claim(s) or which is cited to establish the publication date of another citation or other special reason (as specified)

"O" document referring to an oral disclosure, use, exhibition or other means

"P" document published prior to the international filing date but later than the priority date claimed

"T" later document published after the international filing date or priority date and not in conflict with the application but cited to understand the principle or theory underlying the invention

"X" document of particular relevance;; the claimed invention cannot be considered novel or cannot be considered to involve an inventive step when the document is taken alone

"Y" document of particular relevance;; the claimed invention cannot be considered to involve an inventive step when the document is combined with one or more other such documents, such combination being obvious to a person skilled in the art

"&" document member of the same patent family

Date of the actual completion of the international search	Date of mailing of the international search report
8 March 2023	16/03/2023

Name and mailing address of the ISA/	Authorized officer
European Patent Office, P.B. 5818 Patentlaan 2 NL - 2280 HV Rijswijk Tel. (+31-70) 340-2040, Fax: (+31-70) 340-3016	Werner, Doris

1

Form PCT/ISA/210 (second sheet) (April 2005)

INTERNATIONAL SEARCH REPORT

International application No
PCT/EP2022/086142

C(Continuation). DOCUMENTS CONSIDERED TO BE RELEVANT

Category*	Citation of document, with indication, where appropriate, of the relevant passages	Relevant to claim No.
X	WO 99/26632 A1 (STATENS SERUMINSTITUT [DK]; COHEN PAUL S [US] ET AL.) 3 June 1999 (1999-06-03) claims 8, 1-5 claim 9 claim 11 paragraph [0304] paragraph [0317] -----	1-5,9,11
X	WO 2017/019721 A2 (CONSTELLATION PHARMACEUTICALS INC [US]) 2 February 2017 (2017-02-02) second paragraph; page 11 claim 15 -----	1-5,9,11
Y	MA ANQI ET AL: "Discovery of a first-in-class EZH2 selective degrader", NATURE CHEMICAL BIOLOGY, NATURE PUBLISHING GROUP US, NEW YORK, vol. 16, no. 2, 9 December 2019 (2019-12-09), pages 214-222, XP036996008, ISSN: 1552-4450, DOI: 10.1038/S41589-019-0421-4 [retrieved on 2019-12-09] abstract -----	8

1

INTERNATIONAL SEARCH REPORT

Information on patent family members

International application No
PCT/EP2022/086142

Patent document cited in search report	Publication date	Patent family member(s)	Publication date
WO 2021025148 A1	11-02-2021	AU 2020325143 A1	24-02-2022
		BR 112022001809 A2	29-03-2022
		CA 3148858 A1	11-02-2021
		CN 114173779 A	11-03-2022
		EP 4011452 A1	15-06-2022
		JP WO2021025148 A1	11-02-2021
		KR 20220044679 A	11-04-2022
		TW 202120085 A	01-06-2021
		US 2022280492 A1	08-09-2022
		WO 2021025148 A1	11-02-2021
WO 2017198870 A1	23-11-2017	CA 3024361 A1	23-11-2017
		EP 3458607 A1	27-03-2019
		US 2019284635 A1	19-09-2019
		WO 2017198870 A1	23-11-2017
WO 9926632 A1	03-06-1999	AT 216585 T	15-05-2002
		AU 747288 B2	16-05-2002
		CA 2316340 A1	03-06-1999
		DE 69805100 T2	05-12-2002
		DK 1051180 T3	19-08-2002
		EP 1051180 A1	15-11-2000
		ES 2177089 T3	01-12-2002
		JP 2001523723 A	27-11-2001
		NZ 505233 A	26-07-2002
		US 6165997 A	26-12-2000
		WO 9926632 A1	03-06-1999
WO 2017019721 A2	02-02-2017	US 2020093815 A1	26-03-2020
		WO 2017019721 A2	02-02-2017